This is the accept manuscript of the following article that appeared in final form in Neurobiology of Disease 40(1): 348-359 (2010),
which has been published in final form at https://doi.org/10.1016/j.nbd.2010.06.011.

Engineering *DYRK1A* over-dosage yields Down syndrome-characteristic cortical splicing aberrations

Running title: *Dyrk1A* excess impairs cerebral splicing

Debra Toiber[1]#, Garikoitz Azkona[2,3,4]#, Shani Ben-Ari[1], Nuria Torán[5], Hermona Soreq[1],* and Mara Dierssen[2,3]

[1]Department of Biological Chemistry and Interdisciplinary Center for Neuronal Computation (ICNC), The Hebrew University of Jerusalem, Jerusalem 91904, Israel.

[2]Genes and Disease Program, Centre for Genomic Regulation (CRG), Barcelona Biomedical Research Park (PRBB) and [3]CIBER de Enfermedades Raras (CIBERER), E-08003 Barcelona, Catalonia, Spain.

[4]Department of Neuroscience, University of Basque Country (UPV/EHU), E-48003, Bizkaia, Spain

[5] Section of Pediatric Pathology, Anatomo-Pathology Service, Hospital Universitari Vall d'Hebron, Barcelona, Catalonia, Spain

* To whom correspondence should be addressed: Department of Biological Chemistry; The Hebrew University of Jerusalem; Safra Campus – Givat Ram: Jerusalem 91904 Israel. Tel: 972-2-6585109; Fax: 972-2-652-0258; Email: soreq@cc.huji.ac.il

#These authors contributed equally to this work.

Summary (400 words allowed)

Down syndrome (DS) associates with impaired brain functions, but the underlying mechanism(s) are yet unclear. The "gene dosage" hypothesis predicts that in DS, over-expression of a single gene can impair multiple brain functions through a signal amplification effect due to impaired regulatory mechanism(s). Here, we report findings attributing to impairments in the splicing process such a regulatory role. We have used DS fetal brain samples in search for initial evidence and employed engineered mice with MMU16 partial trisomy (Ts65Dn) or direct excess of the splicing-associated nuclear kinase Dyrk1A, over-dosed in DS for further analyses. We present specific albeit modest changes in the DS brain's splicing machinery with subsequently amplified effects in target transcripts; and we demonstrate that engineered excess of *Dyrk1A* can largely recapitulate these changes. Specifically, in both the fetal DS brains and the *Dyrk1A* over-dose models, we found ample modestly modified splicing-associated transcripts which apparently induced secondary enhancement in exon inclusion of key synaptic transcripts. Thus, DS-reduced levels of the dominant negative TRKBT1 transcript, but not other TRKB mRNA transcripts were accompanied by corresponding decreases in BDNF. Additionally, the DS brains and *Dyrk1A* over-dosage models showed selective changes in the transcripts composition of neuroligin mRNAs as well as reductions in the "synapic" acetylcholinesterase variant *AChE-S* mRNA and corresponding increases in the stress-inducible *AChE-R* mRNA variant, yielding key synaptic proteins with unusual features. In co-transfected cells, *Dyrk1A* over-dosage caused parallel changes in the splicing pattern of an *AChE* mini-gene, suggesting that *Dyrk1A* over-dosage is both essential and sufficient to induce the observed change in the composition of *AChE* mRNA variants. Furthermore, the

Dyrk1A over-dosage animal models showed pronounced changes in the structure of neuronal nuclear speckles, where splicing events take place and in SR proteins phosphorylation known to be required for the splicing process. Together, our findings demonstrate DS-like brain splicing machinery malfunctioning in *Dyrk1A* over-expressing mice. Since individual splicing choices may alter cell fate determination, axon guidance and synaptogenesis, these findings suggest the retrieval of balanced splicing as a goal for DS therapeutic manipulations early in DS development.

Key Words (1-5): Acetylcholinesterase, Down syndrome, Splicing, Neuroligin, Trisomy.

Introduction

Down syndrome (DS; OMIM 190685), the most common genetic disorder leading to mental retardation, is caused by the presence of all or part of an extra copy of chromosome 21 (*HSA21*, for Homo sapiens) (Antonarakis et al., 2004). The neurodevelopmental DS phenotype includes brain abnormalities and moderate mental retardation (Antonarakis and Epstein, 2006; Deutsch et al., 2005). Studies of patients with partial trisomy 21 suggested that the 2-Mb region around locus D21S55 in *HSA21*, DCR-1 (Ahlbom et al., 1996), can be crucial in the pathogenesis of DS (Guimera et al., 1996). Among the genes harbored in this region, those with dosage sensitivity may be of great interest for understanding the neurobiological alterations in DS patients. However, gene copy numbers do not always correspond to protein expression levels (Engidawork and Lubec, 2001; Ferrando-Miguel et al., 2004), suggesting seminal contributions for impaired regulatory mechanisms in DS (Dierssen et al., 2009). A common gene regulatory process, especially relevant for genes that are expressed in the nervous system is pre-mRNA splicing, which affects important regulatory decisions in nearly every step in neuronal development, from neuroblast commitment to synaptic specialization, modulating proteins ranging from transcription factors to cell-adhesion molecules (Li et al., 2007).

Many human disorders are generated by mis-regulation of alternative splicing (Licatalosi and Darnell, 2006; Yamada and Nabeshima, 2004). Even if small, changes in the level of splicing machinery components can perturb the composition of splicing complexes, and thus, induce many changes in downstream processed transcripts. In particular, alternative splicing plays a critical role in the nervous system, where more than 75% of the transcripts are alternatively spliced (Licatalosi and Darnell, 2006; Stamm et al.,

2005). The different variants play essential and sometimes inverse roles in ion channel function, receptor specificity, neuronal cell recognition, neurotransmission, and learning and memory (Li et al., 2007). Mis-regulated alternative splicing is responsible for many nervous system diseases such as Alzheimer's, Parkinson's, Pick's and Huntington's diseases (Licatalosi and Darnell, 2006) but has not yet been explored in other disorders affecting cognition, such as the mental retardation in DS.

Splicing aberrations can directly cause disease, modify the severity of the disease phenotype or be linked with disease susceptibility (Wang and Cooper, 2007). Among the proteins that are involved in the splicing machinery, the members of the SR protein (SRp) family of splicing factors, which contain Ser/Arg-rich domains are primarily involved in mRNA maturation (Hanamura et al., 1998). SRp act as splicing regulatory proteins, binding to exonic splicing enhancer elements and stimulating exon inclusion. SRp family members are mainly named by they size (e.g. SRp20, SRp50, SRp55 etc) and are influenced by protein interactions and posttranslational modifications. Different SRp have different roles depending on combinatorial contributions of cell type, signaling and post-translational modifications. For example, ASF/SF2 (alternative splicing factor/splicing factor 2) affects 5' splice site selection whereas SC35 (Splicing component, 35 kDa) plays an opposite role in the splicing of AChE (Meshorer et al., 2005).

Phosphorylation of SRp is required at the onset of spliceosome assembly (Stamm, 2008). Splicing factors are organized in the highly compartmentalized mammalian nucleus, concentrated in the splicing speckles. These structures (about 25/nucleus) are enriched in splicing factors, pre-messenger RNA, as well as transcription, export and nuclear structural machinery. They are located in the interchromatin regions, close to highly active transcription sites. The speckles are thought to be a "storage" or assembly place for the

splicing machinery. Upon signaling, their components can possibly be mobilized to the target sites. Several kinases and phosphatases are able to modify the splicing machinery, regulating the accessibility of these factors to the splicing events (For a detailed review see (Lamond and Spector, 2003)). A recent example involves the phosphorylation of ASF/SF2, which was suggested to regulate the alternative splicing of tau in DS (Shi et al., 2008).

Expanding this concept, we predicted that splicing efficiency and accuracy at large may be a significant contributor to the DS phenotype and its variability. To challenge this prediction, we comparatively analyzed SRp expression and phosphorylation and the splicing variant profiles of key target genes involved in neurodevelopment and cognition in fetal cerebral cortices from DS carriers and in engineered Dyrk1A over-expression systems.

The Dual-specificity tyrosine phosphorylation-regulated kinase 1A (DYRK1A), a member of an evolutionarily conserved protein kinase family (Becker et al., 1998), has been proposed as an exceptional dosage-sensitive candidate gene for DS. DYRK1A is a proline-directed serine/threonine-specific protein kinase whose activity depends on tyrosine autophosphorylation in the catalytic domain. It maps to the DCR-1, and is highly expressed in fetal and adult brains (Guimera et al., 1999). Multiple reports show involvement of DYRK1A in many different pathways, spanning transcription, translation and signal transduction (Arron et al., 2006; Gwack et al., 2006; Sitz et al., 2004; Yang et al., 2001). In neurons, DYRK1A localizes to both the nucleus and cytoplasm, including neuronal processes and synapses. In the nucleus, it localizes to splicing speckles, and over-expression of active DYRK1A in cultured cells associates with speckles disassembly (Alvarez et al., 2003). Transgenic mice over-expressing *Dyrk1A* (TgDyrk1A), exhibit hyperactivity and impaired neuro-motor development as well as spatial learning and memory (Altafaj et al., 2001; Martinez de Lagran et al., 2004), a phenotype which is

reversible by targeting *Dyrk1A* with AAVshRNA (Ortiz-Abalia et al., 2008). Comparable alterations are found in the MMU16 chromosome 16 partial trisomy murine model of DS, Ts65Dn (Galdzicki et al., 2001), suggesting that *DYRK1A* overexpression in trisomy 21 carriers may contribute to the DS mental retardation and motor anomalies phenotype. The long list of DYRK1A substrates includes Cyclin L2 (de Graaf et al., 2004), SF3b1 (de Graaf et al., 2006) and ASF (Shi et al., 2008), suggesting its possible involvement in the regulation of the splicing machinery (Alvarez et al., 2003; de Graaf et al., 2004; Dean and Dresbach, 2006; Dierssen and de Lagran, 2006). Therefore, we decided to preliminarily investigate the splicing changes induced in the DS brain and compare our findings to those in mice with enforced *Dyrk1A* overexpression. Specifically, we analyzed the splicing machinery at the RNA, protein and phosphorylation levels with a particular focus on genes involved with the molecular basis of learning.

Materials and methods

Human brain samples

Cerebral cortices of fetal brains with or without DS (12 males of each) at 16-19 weeks gestation (Supplementary Table I), were obtained from the fetal tissue bank of Hospital Vall d'Hebron (Barcelona, Spain) and Hospital La Fe (Sabadell, Spain). Samples were obtained between 6 and 12 h post-mortem and were frozen or paraffin embedded. Diagnosis of all cases was genetically and histopathologically confirmed (Dr. N. Torán, Dr. JC Farreras). The inclusion criterion for control samples was that fetal demise was not due to a known genetic cause. Fetal samples were stored at -80ºC until use. DS fetal samples showed elevated DYRK1A protein levels (Supplementary Fig. 1). All experimental procedures were approved by the local ethical committee (CEE-Vall d'Hebrón and CEE-PRBB), and met the guidelines of the local and European regulations.

Animals

The production of transgenic mice over-expressing *Dyrk1A* (TgDyrk1A) has been previously described (Altafaj et al., 2001). Briefly, the original founder was obtained by insertion of the transgene into C57BL/6JXSJL (Charles River, Barcelona, Spain) embryos and the stock is maintained by crossing C57BL/6JXSJL wild type females and transgenic males derived from the original founder. MMU16 Ts65Dn segmental trisomic mice, free from the Rd mutation, were purchased from The Jackson Laboratory (Bar Harbor, Maine, USA). Non-transgenic and disomic littermates served as controls. Both TgDyrk1A and Ts65Dn mice showed elevated protein levels of Dyrk1A compared to strain-matched wild type mice (Supplementary Fig. 1). Animals were housed under 12:12-h light-dark cycle (lights on at 8:00 a.m.) in controlled environmental conditions, 60% of humidity and at

22±2ºC. All animal procedures were approved by the local ethical committee (CEEA-IMIM and CEEA-PRBB), and met the guidelines of the local (law 32/2007) and European regulations (EU directive nº 86/609, EU decree 2001-486) and the Standards for Use of Laboratory Animals nº A5388-01 (NIH). The CRG is authorized to work with genetically modified organisms (A/ES/05/I-13 and A/ES/05/14).

RNA procedures

The RNeasy kit (Qiagen, Valencia, CA) was used as per manufacturer's instructions for RNA extraction. DNase was applied to remove DNA contamination. RNA integrity was confirmed by gel electrophoresis, and RNA concentration and purity was assessed spectrophotometrically. For cDNA synthesis, 0.4 ug RNA was used for each sample (Promega, Madison, WI). The SpliceChip experiment was performed as described previously (Ben-Ari et al., 2006). Quantitative qRT-PCR was performed in duplicates using ABI prism 7900HT and SYBR green master mix (Applied Biosystems, Foster City, CA). ROX, a passive reference dye, was used for signal normalization across the plate, and ß-actin and GAPDH mRNA served as reference transcripts. Annealing temperature was 60ºC for all primers. Serial dilution of samples served to evaluate primer's efficiency and the appropriate cDNA concentration that yields linear changes. Melting curve analysis and amplicons sequencing served to verify the end product. Primers employed are denoted in Supplementary Table 2**.** Transfection and analyses of the human AChE minigene was as previously detailed (Meshorer et al., 2005).

Western blots

Protein content was quantified in postmortem fetal human samples and mouse tissues. Animals were sacrificed, brains rapidly removed and dissected on ice. Tissues were homogenized in lysis buffer (10 mM HEPES pH 7.5, 150 mM NaCl, 1 mM EDTA, 0.1 mM

$MgCl_2$, phosphate-buffered saline (PBS), 0.2% Triton X-100 and a protease inhibitor cocktail (Roche, Mannheim, Germany). After clearance of the lysates by centrifugation (1400xg, 20 min at 4ºC), protein quantification was performed following the BCA Protein Assay Reagent (Pierce, Rockford, IL, USA) protocol. Western blot analysis was performed using 50 μg of protein resolved on a 10% SDS-PAGE and electro-blotting onto nitrocellulose membranes (Hybond-C, Amersham Pharmacia Biotech, Freiburg, Germany). Membranes were blocked with 5% non-fat dry milk or albumin from bovine serum (Sigma, Steinheim, Germany) in Tris-buffered saline including 0.1% Tween-20 (TBS-T) and incubated with the primary antibodies in 5% non-fat dry milk in TBS-T overnight at 4ºC. The following dilutions of primary antibodies were used: mouse anti-ASF/SF2 (1:100; Zymed, CA, USA), anti-Dyrk1A (1:500; Abnova, Heidelberg, Germany), anti-SR proteins (16H3) and (1H4) (1:100 each; Zymed, CA, USA), and goat anti-SC35 (1:200; Santa Cruz, Heidelberg, Germany), rabbit anti-TRKB (1:1000; Santa Cruz), rabbit anti-TRKBT.1 (C13) (1:200; Santa Cruz) and anti-actin (1:2000; Sigma, St Louis, MO, USA). Incubation with horseradish peroxidase (HRP)-conjugated anti- mouse or anti-goat IgG (Pierce, Rockford, IL, USA), followed by enhanced chemiluminescence (ECL, Pierce) assay allowed detection. Quantification involved densitometric analysis of non-saturated films (Quantity One image software).

Co-immunoprecipitation

Cortical extracts (700 μg) were prepared as previously described and subjected to coimmunoprecipitation in lysis buffer containing 0.25% Triton X-100 (overnight, at 4ºC) using rabbit anti-Dyrk1A (kindly provided by Dr. J. Naranjo; CNB, Madrid). After 5 washes in lysis buffer containing 300 mM KCl and 0.25% Triton X-100, proteins were

eluted in SDS sample buffer, resolved in SDS–PAGE and electroblotted onto Immobilon-P (Millipore). Blots were developed using a mouse anti-SR proteins (16H3) (Zymed, CA, USA) or anti-phosphoSer (phosphoserine detection antibody set, Biomol). Proteins were visualized with HRP-conjugated secondary antibodies followed by ECL (West Dura, Pierce).

Immunohistochemistry

Mice were perfused transcardially with 0.1 M PBS, pH 7.4 and then with 4% paraformaldehyde (Sigma, St Louis, MO, USA). After 24h brains were embedded in paraffin, slices (5 μm) were obtained and handled simultaneously during the protocol, to minimize inter-slides variability. Antigen retrieval was performed with Citrate buffer and quenching was performed in human fetal samples with: 0.3% $KMnO_4$ for 4 minutes, deionized water wash, 1% $K_2S_2O_5$ + 1% oxalic acid (20-40 sec), deionized water wash, and 1% $NaBH_4$, 4 min, deionized water wash. Non-specific labelling was blocked for 40 min in Tris 10% serum-blocking solution containing horse and goat serum, 5% each. Mouse anti-ASF/SF2 (1:100; Zymed, CA, USA),anti-SR-phospho proteins (1H4) (1:100; Zymed, CA, USA) and goat anti-SC35 (1:200; Santa Cruz, Heidelberg, Germany), were diluted as for western blots in 2% TBS-milk /5% serum mix and applied for 2h at room temperature or overnight at 4°C. Corresponding biotin-conjugated secondary antibodies with or without Cy3 or Cy2 Conjugates and DAPI served to stain the nucleus. Quantification was done using 4 pictures of each brain area (frontal cortex and the CA1 and dentate gyrus of hippocampus, ImageJ Software). The averages of each picture yielded the final average of the group.

Image analysis

Tissue slices were scanned using an FV-1000 confocal microscope (Olympus, Japan), equipped with an IX81 inverted attachment and an A40X/1.3 oil immersion objective. For DAPI, excitation was 405 and emission 430-470nm; for Cy2, excitation was 488nm and emission 505-525nm. Immuno-staining intensity was quantified by the ImageJ 1 1.33 free software (http://rsb.info.nih.gov/ij/), using the "Analyze tool" mean gray value. Using the "freehand selection" we drew lines around single cells and analyzed 30-300 cells in each picture. Averaged 2-3 empty spots in the tissue served to determine the background for each picture, which was subtracted from each of the values observed for measured cells to normalize light efficiency differences that could occur between different pictures. The total average for a single experiment was composed of 4 different pictures at least from each mouse and 8 mice per group. Standard deviation values were calculated for these averages, to challenge the possibility that a specific change was an outlier which occurred outside the normal range calculated for the other pictures (averages for different mice were used and are depicted in the figures). The data collected from the different cells in each picture was used to derive an average value for that picture. In cell culture experiments, 5-8 different pictures were used to assess each treatment and were analyzed as noted above.

ELISA

BDNF levels were determined using BDNF E_{max}® Immunoassay (Promega, Madison, WI; USA) by the manufacturer's protocol. Briefly, polystyrene-coated ELISA plates were incubated overnight at 4ºC in carbonate-coating buffer containing a polyclonal anti-BDNF antibody. Non-specific binding was blocked by incubating the plate with serum albumin for 1 h at room temperature followed by one wash with 0.1% TBS-T. A standard curve was created from serial dilutions of known concentrations of BDNF ranging from 500-8 pg/ml. After rinsing the plate five times, samples were incubated in the HRP-

conjugated secondary antibody for 2.5 h at room temperature. TMB/peroxidase solution was used as the chromogen to visualize the reaction product. The reaction was allowed to proceed for 10 min and stopped with 1 N hydrochloric acid. Optical density was measured at 450 nm in an ELISA plate reader (Molecular Devices SpectraMax 340 PC, Softmax Pro version 3.1.2).

AChE and BChE activities

Acetylthiocholine (ACTh) hydrolysis rates were measured as detailed (Diamant *et al*., 2006). Readings at 405 nm were repeated at 1-min intervals for 20 min. Non-enzymatic hydrolysis of substrate was subtracted from the total rate of hydrolysis. Enzyme activity was calculated using the molar extinction coefficient for 5-thio-2-nitrobenzoate (13,600 M-1 cm-1) (Ellman et al., 1961).

Statistical Analyses

Data was summarized using SPSS 12.0 as mean ± standard error of mean (S.E.M.). The Mann-Whitney U-test was used for comparing median values whenever two different groups were relatively small (8 samples per karyotype/genotype), assuming non-parametric distribution. The Wilcoxon test was used when one or more observations were "off scale" (more than two standard derivations from the mean). Wilcoxon Matched-Pairs Signed-Ranks was used to compare populations of phosphorylated SR proteins. In all tests, a difference was considered to be significant if the obtained probability reached 0.05.

Results

Aberrant SR protein phosphorylation in the fetal DS cerebral cortex

In immune-blotted extracts from DS brains, ASF/SF2 labeling normalized to actin content was insignificantly lower than in euploid fetal cortices (67.2 ± 524%; $P = 0.08$; see examples in Fig. 1A), SC35 levels were comparable between groups (Fig. 1B) and the DS levels of SRp50 and SRp55 were insignificantly higher (SRp50: 90 ± 36%; $P = 0.09$; SRp55: 157 ± 68%; $P = 0.09$; Fig. 1C). Since splicing is regulated by reversible splicing factor phosphorylation (Stamm, 2008), we predicted that the phosphorylation consequences of these mild SRp changes may be more pronounced in spite of the small group size and heterogeneous nature of the analyzed samples. Compatible with these predictions, immuno-histochemical experiments revealed significantly increased SRp phosphorylation in the DS cerebral cortex (95.1 ± 5.1 %, $P = 0.02$; Fig. 1D), confirmed by Western blots (Wilcoxon Matched-Pairs Signed-Ranks Test; $P < 0.05$), where significant increases were observed in the specific phosphorylation levels of SRp75 (374 ± 43%; $P = 0.04$) and SRp30 (206 ± 9%; $P = 0.02$, Fig. 1E). Thus, splicing protein phosphorylation showed larger differences than protein amounts.

Dyrk1A overexpression mimics the DS-induced changes in splicing machinery

To challenge the hypothesis that *Dyrk1A* over-expression is causally involved with the deregulated splicing machinery in the DS cerebral cortex, pooled RNA samples from the cerebral cortex of 3 TgDyrk1A mice and 3 litter-matched controls were subjected to a spotted microarray carrying ~240 splicing related transcripts (SpliceChip, Supplementary Fig. 2). The levels of over 40 out of 252 tested transcripts were modified by over 40% in

TgDyk1A samples, pointing at *Dyrk1A* as a potential modulator of the splicing machinery. Changes were observed in multiple components of the splicing machinery such as helicases, snRNPs, hnRNPs and SR proteins (Fig. 2A). qRT-PCR validated key changes in samples from individual brains (Fig. 2B). Analysis of the functional groups of genes did not show significant changes (Supplementary Fig. 3), suggesting involvement of multiple specific target transcripts rather than groups of mRNAs.

Changes in individual transcript and protein levels did not always match. Thus ASF/SF2 mRNA showed up-regulation, but immunohistochemistry demonstrated reduced expression of ASF/SF2 in the frontal cortex of TgDyrk1A mice compared to strain-matched controls (66 ± 16.6%; P = 0.05; Fig. 3A), perhaps reflecting micro-RNA blockade of ASF/SF2 mRNA translation. The trisomic Ts65Dn mice showed a reduced expression of ASF/SF2 in the cortex (57.2 ± 4.4%; P = 0.002; Fig. 3B). In contrast, the Srp55 splicing factor was over-expressed in TgDyrk1A cortical extracts (155 ± 12%; P = 0.03) as well as in the Ts65Dn cortex (131 ± 8.6%; P = 0.03; Fig. 3C). Furthermore, Dyrk1A was co-immunoprecipitated from Tg Dyrk1A cortices with an antibody targeting the SR domain of SR proteins, and corresponding immunoblots suggested interaction with SRp55 (Fig. 3D), and its phosphorylation in Ser (Fig. 3E).

Dyrk1A over-dosage enhances SRp phosphorylation and speckle disassembly

In view of the DS changes, we explored if gain of function of the Dyrk1A kinase may affect SRp phosphorylation. In the Dyrk1A frontal cortex, imunohistochemistry revealed increased SR protein phosphorylation (124.1 ± 26.4 %, P = 0.001; Fig. 4A). This result was confirmed by protein blots (Wilcoxon Matched-Pairs Signed-Ranks Test; P < 0.05); where we could distinguish between the different proteins according to their sizes

(see bar graph). Thus SRp150 phosphorylation was significantly increased (179 ± 15%; *P* = 0.04; Fig. 4B). In cortical extracts from Ts65Dn mice, we also observed enhanced SRp phosphorylation, however in these mice SRp30 was the most affected (160 ± 27%; *P* = 0.02; Fig. 4D).

Speckle morphology is an index of the transcriptional state of the cell, but can also be modified by signaling, changing the location of the splicing machinery. To challenge the role of *Dyrk1A* as transcriptional modulator or as a splicing factor regulator, we labeled nuclear speckles in cortical sections from TgDyrk1A and litter-matched control mice with an anti-SC35 antibody. Quantification of SC35 labeled areas revealed no changes upon *in vivo Dyrk1A* over-expression in cortex (Fig. 4D, E). However, the nuclear staining lost the spot pattern, becoming more homogeneous in Dyrk1A mice, and suggesting speckle disassembly or general changes in the nuclear distribution of SC35 (Fig. 4F).

TRKB and AChE splicing variations in the DS fetal cerebral cortex

Changes in TRKB, the high affinity receptor of BDNF were suggested to be causally involved in DS phenotypes (Bimonte-Nelson et al., 2003). TRKB and BDNF are both important in cortical development, activity-dependent synaptic plasticity and memory acquisition and consolidation (Yamada and Nabeshima, 2003). In particular, the TRKBT.1 variant is a dominant negative form of TRKB, lacking the Tyrosine Kinase domain (Rose et al., 2003; Yamada and Nabeshima, 2004), mediating inositol-1,4,5-trisphosphate-dependent calcium release, and playing a role in synaptic plasticity. In DS fetal samples, the *TRKBT.1* variant showed insignificantly lower expression (73 ± 6.6%; *P* = 0.08; Fig. 5B), and once again the effect became significant at the protein level (TRKB-T1: 54 ± 2.7%; *P* = 0.012) where reduced expression of the full length TRKB was also observed (52 ± 6.3%; *P* =

0.012; Fig. 5C). Since the truncated *TRKB*T.1 variant acts as a dominant negative, TRKB becomes more active when the levels of this variant are reduced. This change as well, may initiate downstream effects. For example, a subsequent reduction in the levels of BDNF in DS samples, may reflect a feedback attempt to retrieve normal TRKB signaling (48 ± 11%; $P = 0.03$; Fig. 5D).

The cholinergic neurotransmission system is notably altered in DS patients (Holtzman et al., 1996). Concretely, acetylcholinesterase (AChE) regulates the levels of acetylcholine in the synaptic cleft, and is thus a therapeutic target for DS patients (Kishnani et al., 1999). Alternate promoters and alternative splicing yield different *AChE* variants (Meshorer and Soreq, 2006). Transcripts including the 5' E1e exon and the 3' exon 6 encode the N-terminal apoptotic exon 6 inclusion *N-AChE-S* variant (Toiber et al., 2008), whereas the shorter C-terminal "synaptic" (*AChE-S*) variant is involved in synaptic transmission and neurite growth and the alternative *AChE-R* variant, which includes the 3' intronic I4 region, is involved in distress responses (Meshorer et al., 2002). DS fetal samples showed insignificant changes in *AChE-R* and *AChE-S* expression and hydrolytic AChE activity in control and DS fetal cortical samples (Fig. 5F,G), suggesting that the reported cholinergic deficits in the DS brain develop after birth.

Dyrk1A excess modifies the splicing patterns of synaptic transcripts

Next, we tested if in the adult murine brain, *Dyrk1A* over-dose modifies the splicing pattern of the studied synaptic transcripts. *TrkBT.1* was significantly down-regulated in TgDyrk1A mice, but the full length *TrkB* and the exon inclusion *TrkBT.2* variant both maintained normal levels (Fig. 6A). At the protein level we observed a significant reduction of the full length (23 ± 3.3%; $P = 0.014$) and T.1 isoforms (40 ± 7%; $P = 0.012$; Fig. 6B) in

the transgenic Dyrk1A cortex, but not in Ts65Dn mice (Fig 6C). ELISA showed a significant reduction in BDNF in TgDyrk1A (36 ± 6.4%; $P = 0.04$) but not in Ts65Dn mice (Fig. 6C).

Nevertheless, the levels of the *AChE* common exon 2 and the 5' E1e exon encoding the N-terminal apoptotic variant remained unchanged in the Tg Dyrk1A mouse. In contrast, the *AChE-S* variant was down-regulated, whereas the *AChE-R* variant was significantly up-regulated, attesting to intron 4 retention in the case of the *AChE* gene (Fig. 7A). To find out if *Dyrk1A* over-expression was necessary and sufficient for exerting the observed change, we co-transfected 293T cells with *Dyrk1A* and a mini-*AChE* gene containing the introns and exons of the human sequence. *Dyrk1A* over-expression induced a switch from *AChE-S* to *AChE-R* (Fig. 7B), reminiscent of the change observed in Tg Dyrk1A mice and supporting the previous reports on AChE changes in the DS brain.

Next, we tested neuroligins, cell adhesion molecules involved in cell signaling and in particular, in synaptic function (Dean and Dresbach, 2006). Mutations or alternative splicing of these transcripts affect synaptic fate and function (Levinson and El-Husseini, 2005) and have been implicated in mental retardation (Daoud et al., 2009). In Tg Dyrk1A mice, *Neuroligin 1* showed up-regulation of both variants *A* and *B* in the cerebral cortex (Fig. 7C), whereas its common transcript remained unchanged. The splicing pattern of neuroligin 3 is notably modified in autistic patients (Talebizadeh et al., 2006). In TgDyrk1A mice brains, we identified up-regulation of variant *B*, but neither variant *A* nor the common form of neuroligin 3 (Fig. 7D). Thus, *Dyrk1A* over-dosage was causally involved in shifting synaptic transcripts toward exon inclusion patterns characteristic of brain malfunctioning.

Discussion

The "gene-dosage" hypothesis (Epstein, 1986) predicts that in DS, over-expression of a single gene can impair multiple brain functions through a signal amplification effect. Our combined findings in the fetal DS brain and engineered mouse models and cultured cells with *Dyrk1A* excess present *Dyrk1A* as such a gene, which is primarily involved in monitoring the composition of the splicing machinery. Our findings demonstrate that stable excess of *Dyrk1A* alters the phosphorylation and sub-cellular location of splicing machinery components and modifies key synaptic transcripts, and indicate that *Dyrk1A* over-expression changes the composition of synapses in the mammalian brain. DS is a neuro-developmental brain disorder, and individual splicing choices and splicing regulators contribute to cell-fate determination, axon guidance and synaptogenesis. Therefore, our findings may provide a mechanistic explanation to at least part of the reported cognitive deficiencies in both DS and the *Dyrk1A* over-expressing mice.

DYRK1A is also a transcription regulator, and over-dosage of transcription factors could principally affect the expression levels of splicing factors. In addition, transcription has been coupled to splicing and DYRK1A roles in transcription may also affect splicing. Intriguingly, the levels of splicing factor transcripts in the DS fetal cortex remained largely unchanged, whereas down-stream post-translational changes such as protein levels and patterns of phosphorylation gained significance (e.g. higher SRp75 and SRp30 phosphorylation in the DS fetal brain and in the two Dyrk1A gene dosage murine models). Together, this suggests that DYRK1A activities as a kinase rather than as a transcriptional regulator were primarily involved. The phosphorylation status of SR proteins affects their RNA binding specificity, protein–protein interactions and intracellular distribution, so that

genetic disorders that affect SRp phosphorylation patterns can reciprocally alter splicing, compatible with the Epstein amplification concept. The regulation of splicing is further coupled to transcription (Kornblihtt, 2005), highlighting the combinatorial complexity of the consequences of *Dyrk1A* excess. Correspondingly, *Dyrk1A* excess also altered the splicing patterns of key target transcripts.

That *Dyrk1A* over-expression changed total SR protein properties was indicated by the observed speckle disassembly. Indeed, modifying the sub-nuclear location of splicing factors is known to be a central form of splicing regulation (Melcak et al., 2000). These changes may reflect direct interaction of DYRK1A with splicing factors, as was previously reported for ASF/SF2 (Shi et al., 2008) and Sf3b1/SAP155 (de Graaf et al., 2006). Our current findings suggest that Dyrk1A also interacts directly with SRp55. Consequent to these changes, we found Dyrk1A-mediated exon inclusion events, such as those reported in tauopathies that induce the inclusion of exon 10 in the tau transcript (Shi et al., 2008), or bipolar disorder which is associated with two SNPs located in the neural cell adhesion molecule (NCAM1) gene within a cluster of alternatively spliced exons (Atz et al., 2007). Our findings thus add DYRK1A to other known neuronal-specific splicing modulators, e.g. NOVA2, which modifies the splicing pattern of synapse-related transcripts in a coordinated manner (Ule et al., 2005) and the polypyrimidine-tract-binding protein (PTB) which blocks entry of U2AF into the presplicesomal complex, suppressing inclusion of the neuron-specific c-srcN1 exon in non-neuronal cells (Matsunaga et al., 1993).

Downstream target genes we tested, include *Neuroligin 1* and *3*, *TRKB and AChE*. That the changes induced by *DYRK1A* over-expression, primarily involved exon inclusions can have a profound effect on Neuroligin-Neurexin interactions. Specifically, Neuroligin splicing dictates the formation of inhibitory or excitatory synapses through changing its

binding characteristics with Neurexin variants (Dean and Dresbach, 2006), as was suggested to be the case in autism (Boucard et al., 2005). Downstream changes, induced by those occurring in Neuroligin would predictably change the binding affinity of the Neuroligin protein products, which can modify synaptic composition. Recently, chronic systemic treatment of Ts65Dn mice with GABAA antagonists at non-epileptic doses caused persistent post-drug recovery of cognition and long-term potentiation (Fernandez et al., 2007). This and other observations (Kurt et al., 2000) indicate the existence of a relative excess of inhibitory synapses in these mice, compatible with our Dyrk1A-related changes in neuroligin alternative variants.

In DS fetal samples, we detected lower expression of BDNF and of the full length TRKB isoform, which can compromise cell proliferation and differentiation. In previous studies, changes in the lamination of the neorcortex of DS fetal brains, were correlated with a significant reduction of full length TRKB (Wisniewski, 1990). In our hands, a trend towards lower expression of the truncated TRKBT.1 variant was accompanied by a significant decrease at the protein level. BDNF reduction was also observed in the cortex of Ts65Dn mice, and BDNF mRNA was reduced in the Down Syndrome hippocampus. The diminutions in mice correlated with working memory errors; in addition, the low levels were corrected in the YACtg152F7 mice by the use of Green tea polyphenols (DYRK1A inhibitors)(please add ref 12642175 and 19242551) Likewise, reducing the levels of AChE-S impairs neuritogenesis, compatible with the neuritogenesis alterations observed in DS patients (Dierssen and Ramakers, 2006). Inversely, elevated levels of the stress-induced *AChE-R* splicing variant have been observed in the frontal cortex of over 60 years old DS brains, and in AD patients (Darreh-Shori et al., 2004). That the slight variations in the *AChE* splicing pattern in DS fetal cortices did not lead to changes in AChE's catalytic

activity suggests stable cholinergic metabolism in DS individuals at early developmental stages, as was previously proposed (Brooksbank et al., 1989; Kish et al., 1989).

Additional examples of genes regulated by DYRK1A at the transcription level may highlight specific motif(s) that might be present in their promoter region. Similarly, wider scope screening could be useful to find common motifs in the alternatively spliced target genes, and decipher if this splicing misregulation is synaptic-related, brain-specific, or if it enables wider and more robust changes. While the effect of DYRK1A is likely not limited to brain functions, the higher diversity of splicing variations in the central nervous system predicts that splicing changes might affect brain development and function in a more pronounced manner than other organs (Licatalosi and Darnell, 2006). Others reported that DYRK1A mis-regulation leads to impairments in brain function (Altafaj et al., 2001; Fotaki et al., 2002; Martinez de Lagran et al., 2004), and that its over-expression is related to pathological aging (Ferrer et al., 2005). Our current work suggests that DYRK1A regulates the splicing machinery in general, at both the post-transcriptional and the posttranslational levels, which helps to explain those observations. Recent discoveries point at a role for alternative splicing machinery in cancer (Kim et al., 2008; Soreq et al., 2008). Compatible with this, DS carriers are prone to leukemia (Zwaan et al., 2008), which could be related to alterations in the hematopoietic splicing machinery.

Acknowledgments

We thank Prof. J.R. Naranjo and Dr. B. Mëlstrom for their kind help in immunoprecipitation experiments and the *Dyrk1A* plasmid.

Funding

This research was supported by the European Union (LSH-2004-1.1.5-3 and STREP (LSHG-CT-2006-037277), The German, Israeli and Spanish Ministries of Science and the German-Israel Project, DIP-G 3.2, The Hebrew University's Interdisciplinary Center for Neuronal Computation (ICNC), The CIBERER Foundation, UK and Jerome Lejeune Foundation, France. G. Azkona received a fellowship (BFI05.48) from the Basque Country Government, Spain.

References

Ahlbom, B. E., et al., 1996. Molecular analysis of chromosome 21 in a patient with a phenotype of Down syndrome and apparently normal karyotype. Am J Med Genet. 63, 566-72.

Altafaj, X., et al., 2001. Neurodevelopmental delay, motor abnormalities and cognitive deficits in transgenic mice overexpressing Dyrk1A (minibrain), a murine model of Down's syndrome. Hum Mol Genet. 10, 1915-23.

Alvarez, M., et al., 2003. DYRK1A accumulates in splicing speckles through a novel targeting signal and induces speckle disassembly. J Cell Sci. 116, 3099-107.

Antonarakis, S. E., Epstein, C. J., 2006. The challenge of Down syndrome. Trends Mol Med. 12, 473-9.

Antonarakis, S. E., et al., 2004. Chromosome 21 and down syndrome: from genomics to pathophysiology. Nat Rev Genet. 5, 725-38.

Arron, J. R., et al., 2006. NFAT dysregulation by increased dosage of DSCR1 and DYRK1A on chromosome 21. Nature. 441, 595-600.

Atz, M. E., et al., 2007. NCAM1 association study of bipolar disorder and schizophrenia: polymorphisms and alternatively spliced isoforms lead to similarities and differences. Psychiatr Genet. 17, 55-67.

Becker, W., et al., 1998. Sequence characteristics, subcellular localization, and substrate specificity of DYRK-related kinases, a novel family of dual specificity protein kinases. J Biol Chem. 273, 25893-902.

Ben-Ari, S., et al., 2006. Modulated splicing-associated gene expression in P19 cells expressing distinct acetylcholinesterase splice variants. J Neurochem. 97 Suppl 1, 24-34.

Bimonte-Nelson, H. A., et al., 2003. Frontal cortex BDNF levels correlate with working memory in an animal model of Down syndrome. Behav Brain Res. 139, 47-57.

Boucard, A. A., et al., 2005. A splice code for trans-synaptic cell adhesion mediated by binding of neuroligin 1 to alpha- and beta-neurexins. Neuron. 48, 229-36.

Brooksbank, B. W., et al., 1989. Neuronal maturation in the foetal brain in Down's syndrome. Early Hum Dev. 18, 237-46.

Daoud, H., et al., 2009. Autism and Nonsyndromic Mental Retardation Associated with a De Novo Mutation in the NLGN4X Gene Promoter Causing an Increased Expression Level. Biol Psychiatry.

Darreh-Shori, T., et al., 2004. Long-lasting acetylcholinesterase splice variations in anticholinesterase-treated Alzheimer's disease patients. J Neurochem. 88, 1102-13.

de Graaf, K., et al., 2006. The protein kinase DYRK1A phosphorylates the splicing factor SF3b1/SAP155 at Thr434, a novel in vivo phosphorylation site. BMC Biochem. 7, 7.

de Graaf, K., et al., 2004. Characterization of cyclin L2, a novel cyclin with an arginine/serine-rich domain: phosphorylation by DYRK1A and colocalization with splicing factors. J Biol Chem. 279, 4612-24.

Dean, C., Dresbach, T., 2006. Neuroligins and neurexins: linking cell adhesion, synapse formation and cognitive function. Trends Neurosci. 29, 21-9.

Deutsch, S., et al., 2005. Gene expression variation and expression quantitative trait mapping of human chromosome 21 genes. Hum Mol Genet. 14, 3741-9.

Dierssen, M., de Lagran, M. M., 2006. DYRK1A (Dual-Specificity Tyrosine-Phosphorylated and -Regulated Kinase 1A): A Gene with Dosage Effect During Development and Neurogenesis. ScientificWorldJournal. 6, 1911-22.

Dierssen, M., et al., 2009. Aneuploidy: from a physiological mechanism of variance to Down syndrome. Physiol Rev. 89, 887-920.

Dierssen, M., Ramakers, G. J., 2006. Dendritic pathology in mental retardation: from molecular genetics to neurobiology. Genes Brain Behav. 5 Suppl 2, 48-60.

Ellman, G. L., et al., 1961. A new and rapid colorimetric determination of acetylcholinesterase activity. Biochem. Pharmacol. 7, 88-95.

Engidawork, E., Lubec, G., 2001. Protein expression in Down syndrome brain. Amino Acids. 21, 331-61.

Epstein, C. J., 1986. Developmental genetics. Experientia. 42, 1117-28.

Fernandez, F., et al., 2007. Pharmacotherapy for cognitive impairment in a mouse model of Down syndrome. Nat Neurosci. 10, 411-3.

Ferrando-Miguel, R., et al., 2004. Protein levels of genes encoded on chromosome 21 in fetal Down Syndrome brain (Part V): overexpression of phosphatidyl-inositol-glycan class P protein (DSCR5). Amino Acids. 26, 255-61.

Ferrer, I., et al., 2005. Constitutive Dyrk1A is abnormally expressed in Alzheimer disease, Down syndrome, Pick disease, and related transgenic models. Neurobiol Dis. 20, 392-400.

Fotaki, V., et al., 2002. Dyrk1A haploinsufficiency affects viability and causes developmental delay and abnormal brain morphology in mice. Mol Cell Biol. 22, 6636-47.

Galdzicki, Z., et al., 2001. On the cause of mental retardation in Down syndrome: extrapolation from full and segmental trisomy 16 mouse models. Brain Res Brain Res Rev. 35, 115-45.

Guimera, J., et al., 1999. Human minibrain homologue (MNBH/DYRK1): characterization, alternative splicing, differential tissue expression, and overexpression in Down syndrome. Genomics. 57, 407-18.

Guimera, J., et al., 1996. A human homologue of Drosophila minibrain (MNB) is expressed in the neuronal regions affected in Down syndrome and maps to the critical region. Hum Mol Genet. 5, 1305-10.

Gwack, Y., et al., 2006. A genome-wide Drosophila RNAi screen identifies DYRK-family kinases as regulators of NFAT. Nature. 441, 646-50.

Hanamura, A., et al., 1998. Regulated tissue-specific expression of antagonistic pre-mRNA splicing factors. Rna. 4, 430-44.

Holtzman, D. M., et al., 1996. Developmental abnormalities and age-related neurodegeneration in a mouse model of Down syndrome. Proc Natl Acad Sci U S A. 93, 13333-8.

Kim, E., et al., 2008. Insights into the connection between cancer and alternative splicing. Trends Genet. 24, 7-10.

Kish, S., et al., 1989. Down's syndrome individuals begin life with normal levels of brain cholinergic markers. J Neurochem. 52, 1183-7.

Kishnani, P. S., et al., 1999. Cholinergic therapy for Down's syndrome. Lancet. 353, 1064-5.

Kornblihtt, A. R., 2005. Promoter usage and alternative splicing. Curr Opin Cell Biol. 17, 262-8.

Kurt, M. A., et al., 2000. Synaptic deficit in the temporal cortex of partial trisomy 16 (Ts65Dn) mice. Brain Res. 858, 191-7.

Lamond, A. I., Spector, D. L., 2003. Nuclear speckles: a model for nuclear organelles. Nat Rev Mol Cell Biol. 4, 605-12.

Levinson, J. N., El-Husseini, A., 2005. Building excitatory and inhibitory synapses: balancing neuroligin partnerships. Neuron. 48, 171-4.

Li, Q., et al., 2007. Neuronal regulation of alternative pre-mRNA splicing. Nat Rev Neurosci. 8, 819-31.

Licatalosi, D. D., Darnell, R. B., 2006. Splicing regulation in neurologic disease. Neuron. 52, 93-101.

Martinez de Lagran, M., et al., 2004. Motor phenotypic alterations in TgDyrk1a transgenic mice implicate DYRK1A in Down syndrome motor dysfunction. Neurobiol Dis. 15, 132-42.

Matsunaga, T., et al., 1993. Expression of alternatively spliced src messenger RNAs related to neuronal differentiation in human neuroblastomas. Cancer Res. 53, 3179-85.

Melcak, I., et al., 2000. Nuclear pre-mRNA compartmentalization: trafficking of released transcripts to splicing factor reservoirs. Mol Biol Cell. 11, 497-510.

Meshorer, E., et al., 2005. SC35 promotes sustainable stress-induced alternative splicing of neuronal acetylcholinesterase mRNA. Mol Psychiatry. 10, 985-97.

Meshorer, E., et al., 2002. Alternative splicing and neuritic mRNA translocation under long-term neuronal hypersensitivity. Science. 295, 508-12.

Meshorer, E., Soreq, H., 2006. Virtues and woes of AChE alternative splicing in stress-related neuropathologies. Trends Neurosci. 29, 216-24.

Ortiz-Abalia, J., et al., 2008. Targeting Dyrk1A with AAVshRNA attenuates motor alterations in TgDyrk1A, a mouse model of Down syndrome. Am J Hum Genet. 83, 479-88.

Rose, C. R., et al., 2003. Truncated TrkB-T1 mediates neurotrophin-evoked calcium signalling in glia cells. Nature. 426, 74-8.

Shi, J., et al., 2008. Increased Dosage of Dyrk1A Alters Alternative Splicing Factor (ASF)-regulated Alternative Splicing of Tau in Down Syndrome. J Biol Chem. 283, 28660-28669.

Sitz, J. H., et al., 2004. Dyrk1A potentiates steroid hormone-induced transcription via the chromatin remodeling factor Arip4. Mol Cell Biol. 24, 5821-34.

Soreq, L., et al., 2008. Advanced microarray analysis highlights modified neuro-immune signaling in nucleated blood cells from Parkinson's disease patients. J Neuroimmunol. 201-202, 227-36.

Stamm, S., 2008. Regulation of alternative splicing by reversible protein phosphorylation. J Biol Chem. 283, 1223-7.

Stamm, S., et al., 2005. Function of alternative splicing. Gene. 344, 1-20.

Talebizadeh, Z., et al., 2006. Novel splice isoforms for NLGN3 and NLGN4 with possible implications in autism. J Med Genet. 43, e21.

Toiber, D., et al., 2008. N-acetylcholinesterase-induced apoptosis in Alzheimer's disease. PLoS ONE. 3, e3108.

Ule, J., et al., 2005. Nova regulates brain-specific splicing to shape the synapse. Nat Genet. 37, 844-52.

Wang, G. S., Cooper, T. A., 2007. Splicing in disease: disruption of the splicing code and the decoding machinery. Nat Rev Genet. 8, 749-61.

Wisniewski, K. E., 1990. Down syndrome children often have brain with maturation delay, retardation of growth, and cortical dysgenesis. Am J Med Genet Suppl. 7, 274-81.

Yamada, K., Nabeshima, T., 2003. Brain-derived neurotrophic factor/TrkB signaling in memory processes. J Pharmacol Sci. 91, 267-70.

Yamada, K., Nabeshima, T., 2004. Interaction of BDNF/TrkB signaling with NMDA receptor in learning and memory. Drug News Perspect. 17, 435-8.

Yang, E. J., et al., 2001. Protein kinase Dyrk1 activates cAMP response element-binding protein during neuronal differentiation in hippocampal progenitor cells. J Biol Chem. 276, 39819-24.

Zwaan, M. C., et al., 2008. Acute leukemias in children with Down syndrome. Pediatr Clin North Am. 55, 53-70, x.

Figure Legends:

Figure 1. SR proteins levels and phosphorylation in DS fetal cerebral cortex. Upper panels: SR proteins; lower panels: posterior densitometric quantification graphed as percentage of control values from cerebral cortices of fetal brains. Actin was used as loading control. **A.** Representative protein blot of ASF/SF2 **B.** SC35 and **C.** SRp50 and SRp55. **D.** Representative confocal images of cortical fetal cells immunostained with an anti-SRp-phospho (1H4) antibody, showing a higher expression of phosphorylated SR proteins in DS cortices compared to controls. Left panel: controls, Right panel: DS; Scale bar = 50 µm. Right upper insert: higher magnification (Scale bar = 5 µm). **E.** Representative protein blot of phosphorylated SR proteins and densitometric quantification graphed as percentage of control values from cerebral cortex of normal fetal samples. Actin was used as loading control. N = 4 per Karyotype for immunohistochemistry analysis and 8 per Karyotype per protein blot analysis. White bars: controls; black bars: DS fetal cortical tissues. Data are expressed as mean ± S.E.M. * $P < 0.05$. Mann-Whitney's U test.

Figure 2. *Dyrk1A* over-expression modifies the levels of splicing machinery transcripts

A. Splice Chip results for TgDyrk1A cortices compared to strain matched controls. Bar graphs represent genes related to splicing that were up/down regulated significantly in both experiments. Data are presented as log 2 scale showing increase or decrease from control mice (log 2 <-0.5 or >0.5). N = 3 per genotype. **B.** Bar graphs represent percent of change from control in qRT-PCR of individual brain samples for the noted transcripts. N = 6 per genotype. Black bars represent TgDyrk1A and white bars control mice. * $P < 0.05$. Mann-Whitney U test.

Figure 3. Dyrk1A over-expression modifies splicing factor protein levels

A. Immunohistochemistry for ASF/SF2 and its quantification of TgDyrk1A frontal cortex. **B.** Protein blot quantification for ASF/SF2 of TgDyrk1A and Ts65Dn mice cortex. **C.** Western blot quantification for SRp55 of TgDyrk1A and Ts65Dn mice cortex. **D.** Co-immunoprecipitation of mouse protein brains extracts with anti-Dyrk1A, showing SRp55 interaction. **E.** Co-immunoprecipitation showing SRp55 phosphorylation at Ser. N = 4 per genotype for immunohistochemistry analysis and 8 per genotype per Wester blot analysis.. Data are expressed as mean ± S.E.M. * $P < 0.05$, ** $P < 0.01$. Mann-Whitney U test.

Figure 4. Phosphorylation of SR proteins in cortex of TgDyrk1A and Ts65Dn

A. Immunohistochemistry of phosphorylated SR proteins in cortices from control and TgDyrk1A mice. **B.** Blot quantification for phosphorylated SR proteins of TgDyrk1A. **C.** Phosphorylated SR protein blot of cortex extracts from Ts65Dn mice. **D.** Inmunohistochemistry of frontal cortex and **E**. Blot using SC35 antibody in TgDyrk1A and control cortices. **F.** Inmunohistochemistry showing speckles disassembly in the TgDyrk1A cortex. N = 4 per genotype for immunohistochemistry analysis and 8 per genotype per blot analysis.. Data expressed as mean ± S.E.M. * $P < 0.05$, ** $P < 0.01$. Mann-Whitney U test.

Figure 5. TRKB-BDNF system and *AChE* splicing variants and catalytic activity in DS fetal cerebral cortex.

A. Schematic representation of the *NTRK2* (*TRKB)* gene including the position of primers used for each variant (pink: the exon specific for *TRKBT.1* variant; green: the exon specific for *TRKBT.2*). **B.** Analysis of *TRKB* splicing variants. Changes in qRT-PCR are shown as percent from control for the different variants of the tested transcripts. **C.** Representative

blot of *TRKB* isoforms and densitometric quantification graphed as percentage of control indicating lower expression of TRKB full length (F.L.) and TRKBT.1 isoforms in the cerebral cortex of DS fetal samples. Actin was used as loading control. **D.** BDNF quantification by ELISA. **E.** Schematic representation of the *AChE* gene including the position of primers used for each variant (indicated by coloured arrows, red: E1 exon that encodes the N-terminal fragment; blue: I4 intron that encodes the C-terminal *AChE-R* variant; green: E6 exon that encodes the C-terminal *AChE-S* variant). **F.** Analysis by qRT-PCR of *AChE* splicing variants. Note a non-significant trend towards upregulation of *AChE-R*, and downregulation of *AChE-S*. **G.** AChE and BChE activity was not different between groups. White bars: controls; black bars: DS fetal cortical tissues. N = 8 per karyotype. Data expressed as mean ± S.E.M. * $P < 0.05$. Mann-Whitney U-test.

Figure 6. The TRKB-BDNF system in *Dyrk1A* overexpressing cortices. A. *TrkB* splicing variants expression by qRT-PCR. **B.** TRKB full length (F.L.) and TRKBT.1 and BDNF quantities in TgDyrk1A. **C.** TRKB full length (F.L.) and TRKBT.1 isoforms expression by blot and BDNF quantification in Ts65Dn mice. N = 4 per genotype. Data expressed as mean ± S.E.M. * $P < 0.05$. Mann-Whitney U test.

Figure 7. Splicing modifications target neuronal transcripts. A. *Ache* splicing variants (qRT-PCR). **B.** Co-transfecting 293T cells with the AChE mini-gene and *DYRK1A* reduced AChE-S and increased AChE-R compared to controls. **C.** Splicing variants of *neuroligin 1* and **D.** Splicing variants of *neuroligin 3* by qRT-PCR . N =4 per genotype. Data expressed as mean ± S.E.M. * $P < 0.05$. Mann-Whitney U test.

Figure 8. Proposed mechanism of DYRK1A effects on mental retardation. A. DYRK1A over-expression; **B.** Imbalanced splicing machinery, hyperphosphorylated SR proteins and speckles disassembly; **C.** Changes in SRp; **D.** Changes in the nuclear speckles; **E.** Changes in target synapses. **F.** All of these changes together may affect **G.** Synaptic plasticity and **H.** Spine composition and properties.

Supplementary Figures

Supplementary Figure 1. Dyrk1A quantification by blot. TgDyrk1A, Ts65Dn and DS fetal cerebral cortex samples showed higher Dyrk1A expression levels. (n =4 per genotype/karyotype). Data expressed as mean ± S.E.M. * $P < 0.05$. Mann-Whitney U test.

Supplementary Figure 2. SpliceChip results

Supplementary Figure 3. Functional analysis of Splice Chip

A

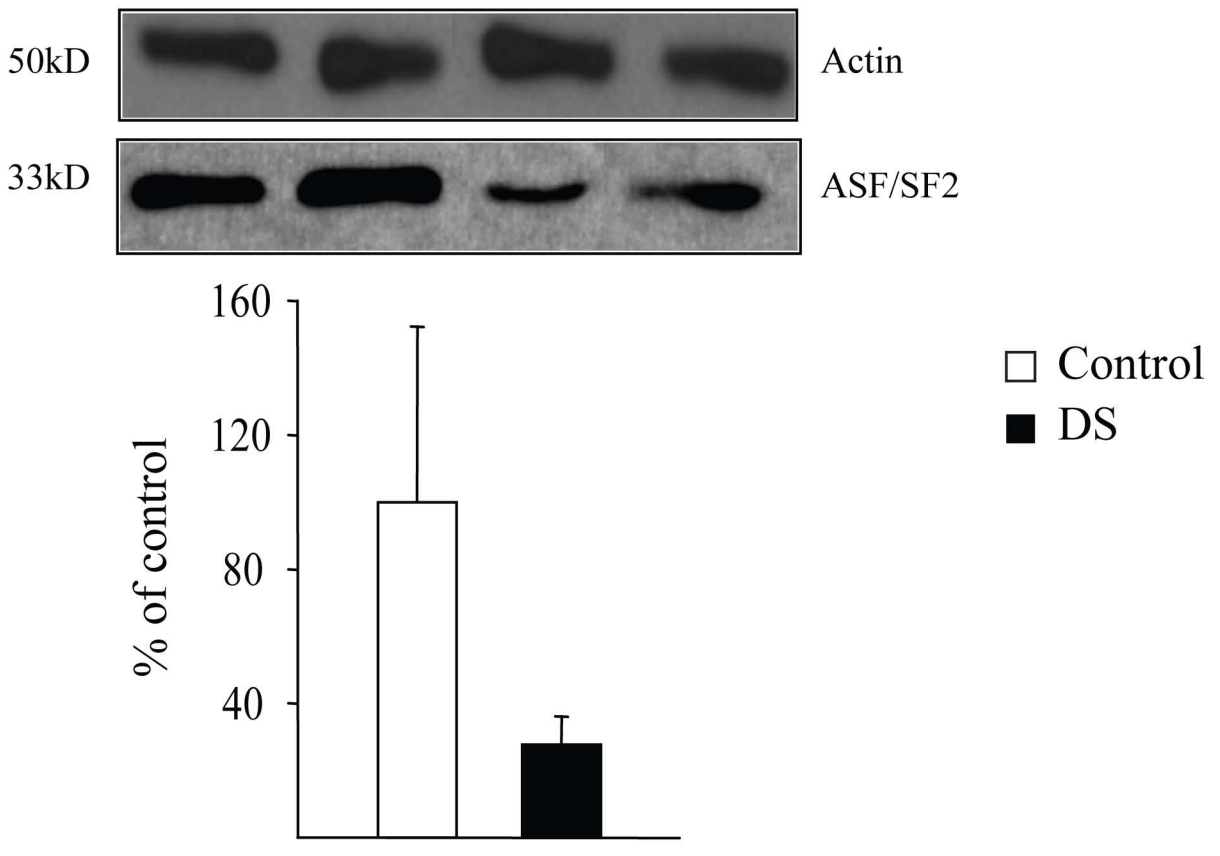
Control
DS
50kD
Actin
33kD
ASF/SF2
% of control
160
120
80
40
Control
DS

B

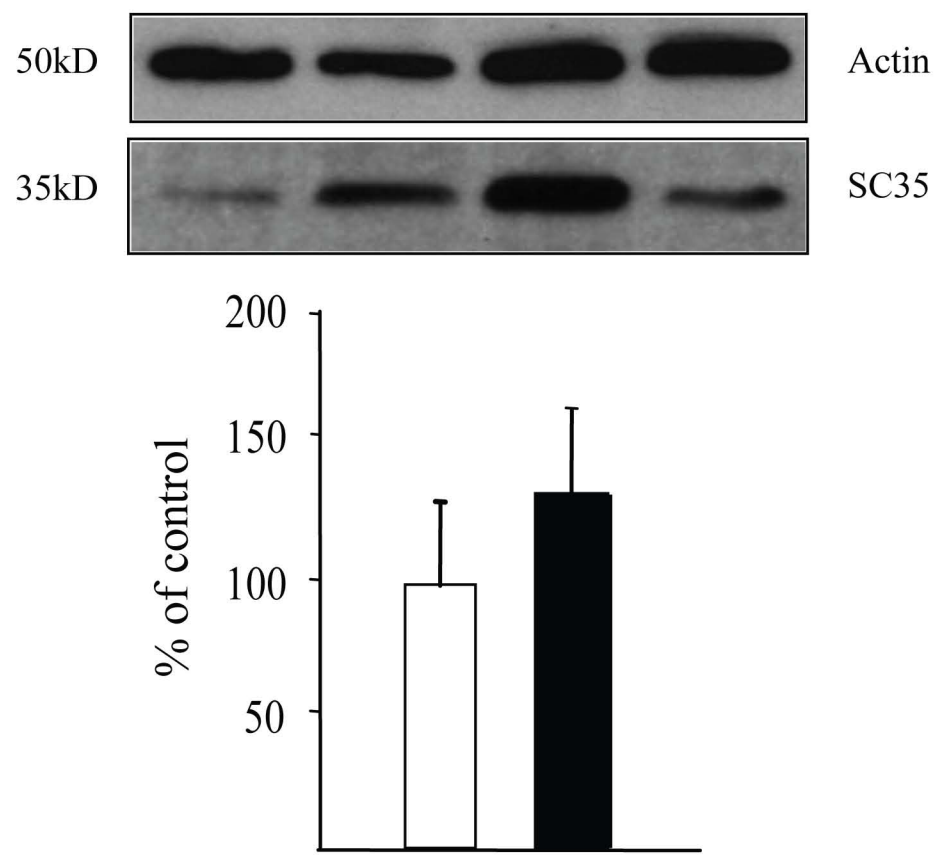
Control
DS
50kD
Actin
35kD
SC35
% of control
200
150
100
50

C

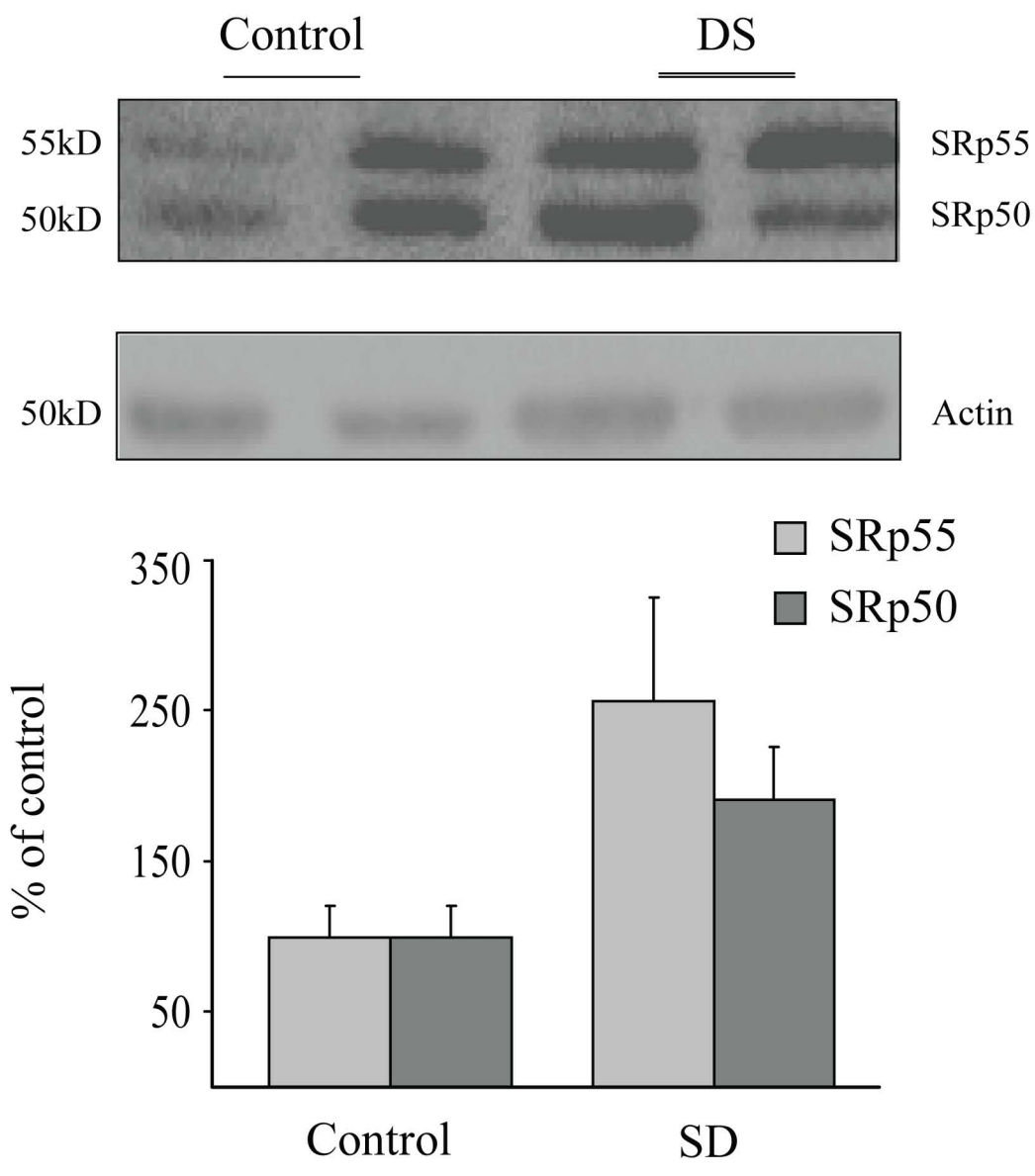
Control
DS
55kD
SRp55
50kD
SRp50
50kD
Actin
SRp55
SRp50
% of control
350
250
150
50
Control
SD

D

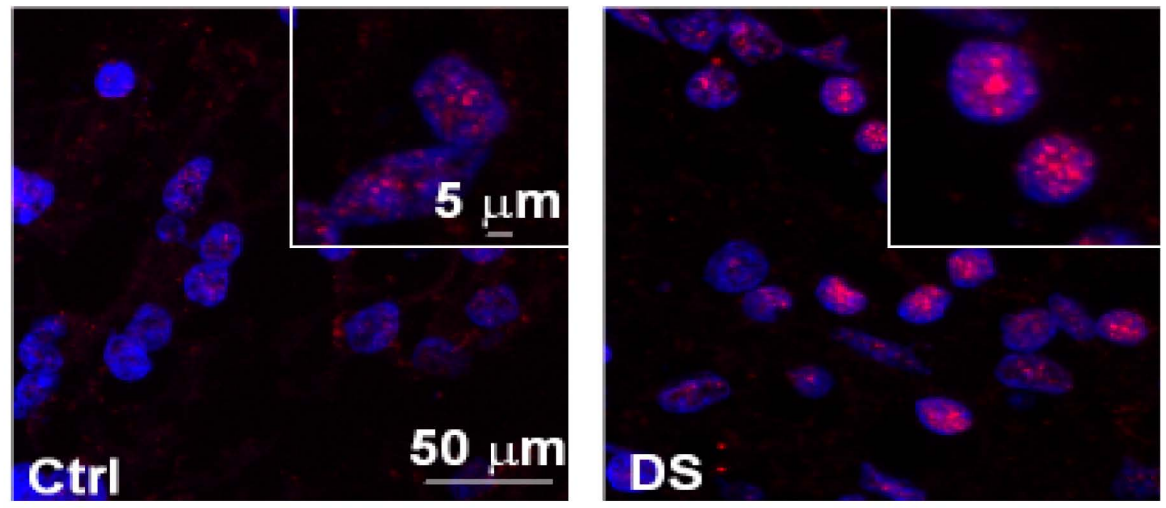
5 μm
50 μm
Ctrl
DS

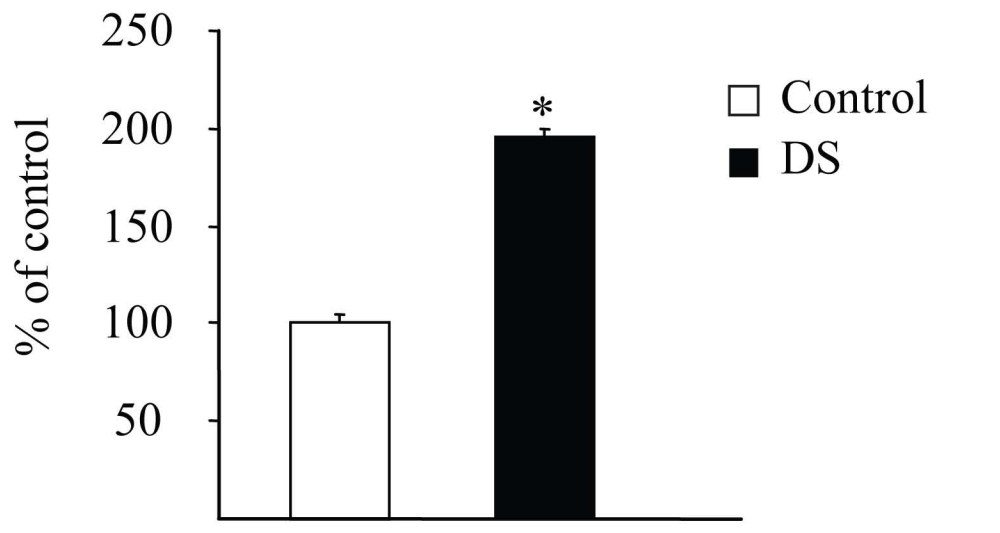
% of control
250
200
150
100
50
*
Control
DS

E

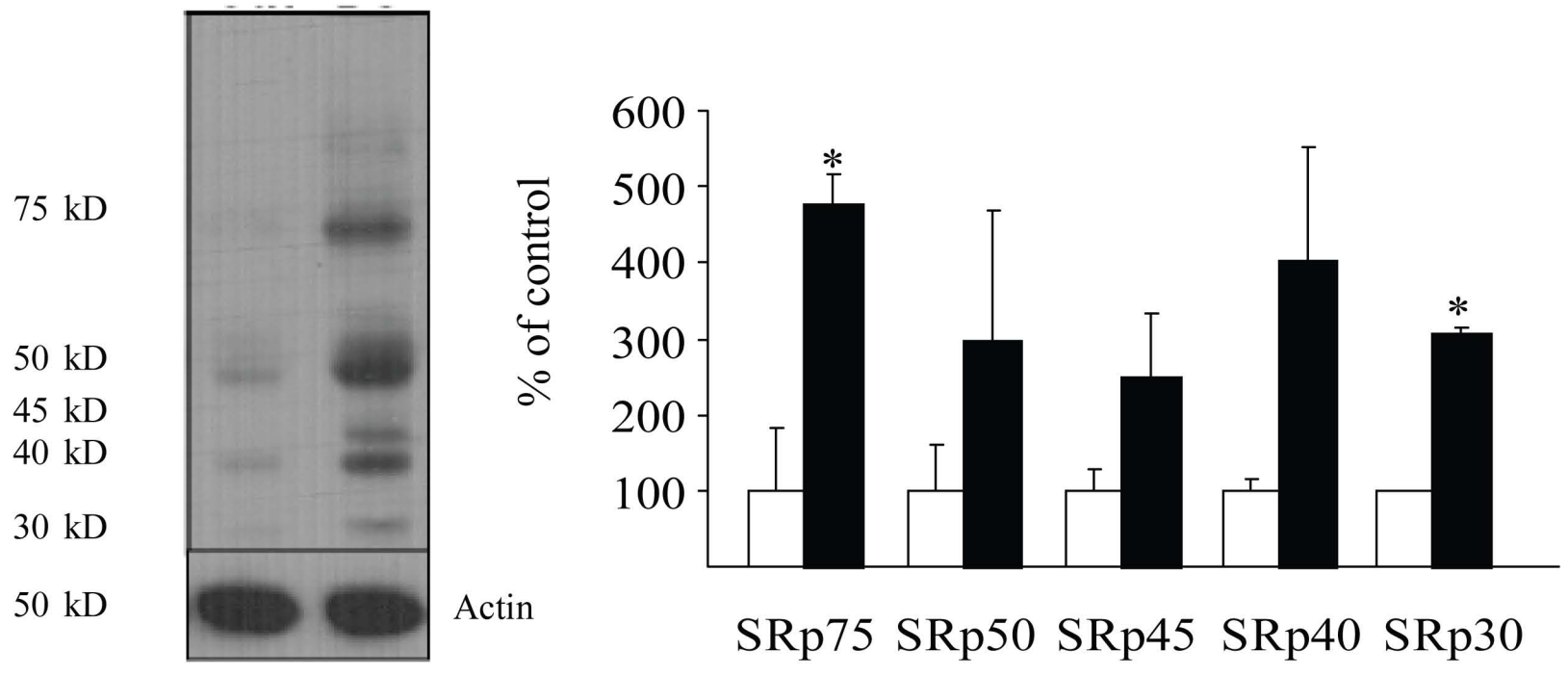
75 kD
50 kD
45 kD
40 kD
30 kD
50 kD
Actin
% of control
600
500
400
300
200
100
*
*
SRp75
SRp50
SRp45
SRp40
SRp30

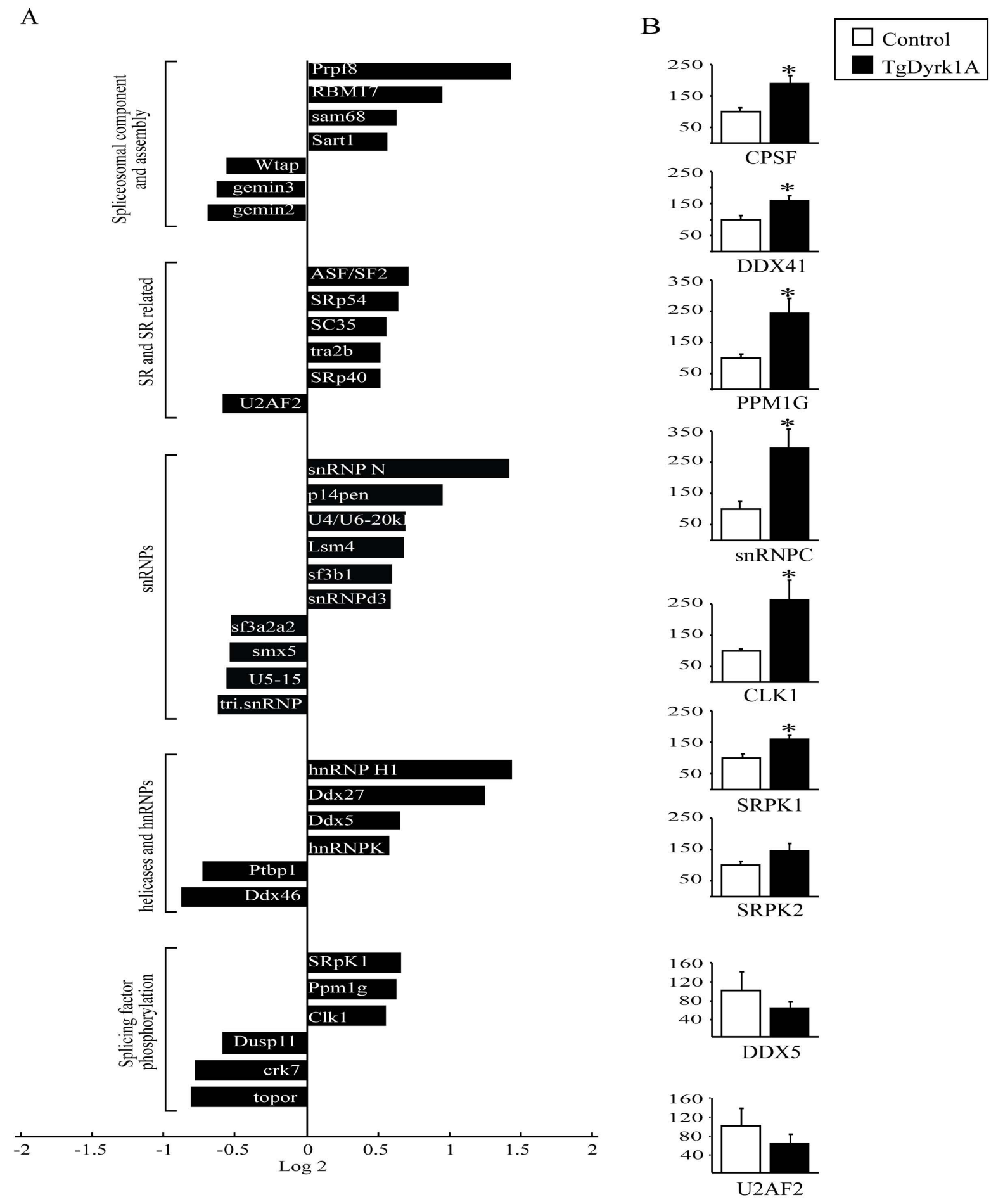
A
Spliceosomal component and assembly
SR and SR related
snRNPs
helicases and hnRNPs
Splicing factor phosphorylation
Prpf8
RBM17
sam68
Sart1
Wtap
gemin3
gemin2
ASF/SF2
SRp54
SC35
tra2b
SRp40
U2AF2
snRNP N
p14pen
U4/U6-20k
Lsm4
sf3b1
snRNPd3
sf3a2a2
smx5
U5-15
tri.snRNP
hnRNP H1
Ddx27
Ddx5
hnRNPK
Ptbp1
Ddx46
SRpK1
Ppm1g
Clk1
Dusp11
crk7
topor
-2
-1.5
-1
-0.5
0
0.5
1
1.5
2
Log 2
B
Control
TgDyrk1A
250
150
50
CPSF
DDX41
350
PPM1G
snRNPC
CLK1
SRPK1
SRPK2
160
120
80
40
DDX5
U2AF2
*

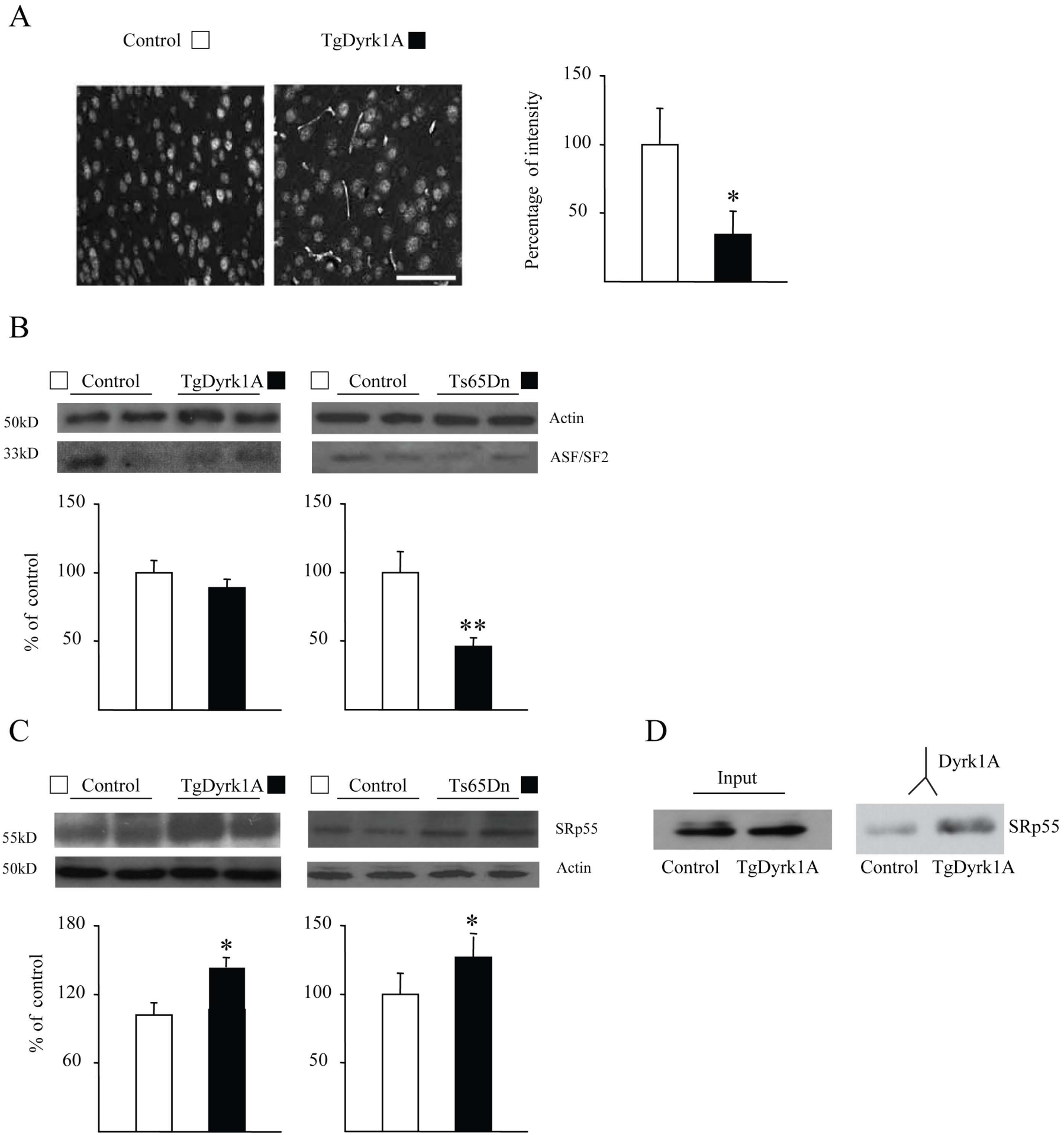
A
Control
TgDyrk1A
Percentage of intensity
150
100
50
*
B
Control
TgDyrk1A
Control
Ts65Dn
50kD
33kD
Actin
ASF/SF2
% of control
150
100
50
**
C
Control
TgDyrk1A
Control
Ts65Dn
55kD
50kD
SRp55
Actin
% of control
180
120
60
150
100
50
*
*
D
Input
Dyrk1A
SRp55
Control
TgDyrk1A
Control
TgDyrk1A

A

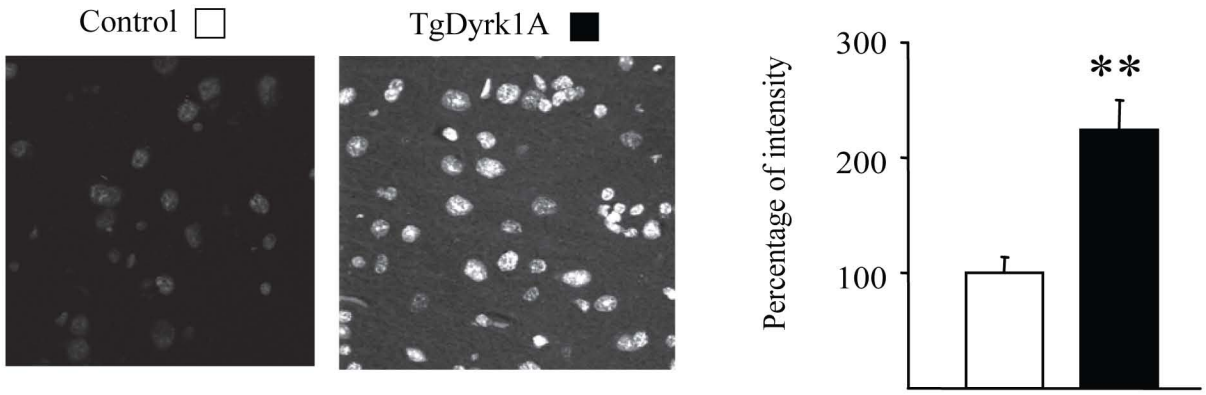
Control
TgDyrk1A
Percentage of intensity
300
200
100
**

B

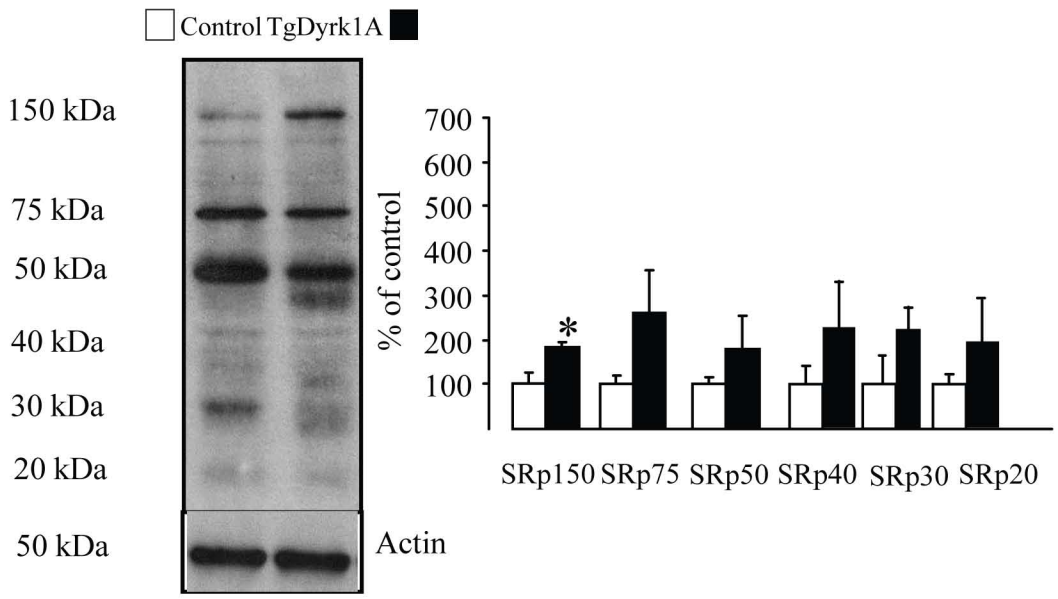
Control TgDyrk1A
150 kDa
75 kDa
50 kDa
40 kDa
30 kDa
20 kDa
50 kDa
Actin
% of control
700
600
500
400
300
200
100
*
SRp150 SRp75 SRp50 SRp40 SRp30 SRp20

C

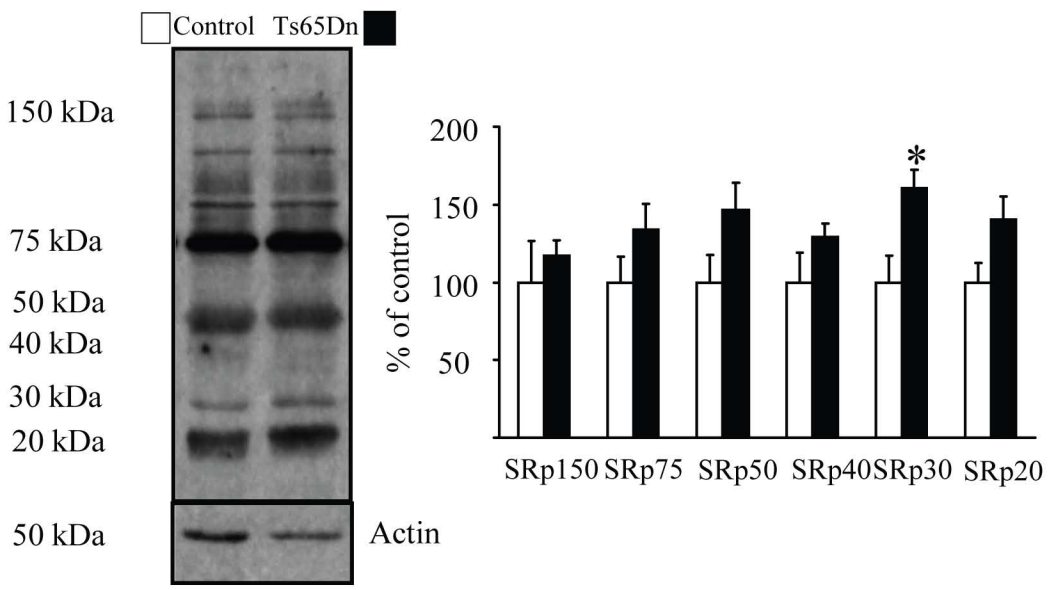
Control Ts65Dn
150 kDa
75 kDa
50 kDa
40 kDa
30 kDa
20 kDa
50 kDa
Actin
% of control
200
150
100
50
*
SRp150 SRp75 SRp50 SRp40 SRp30 SRp20

D

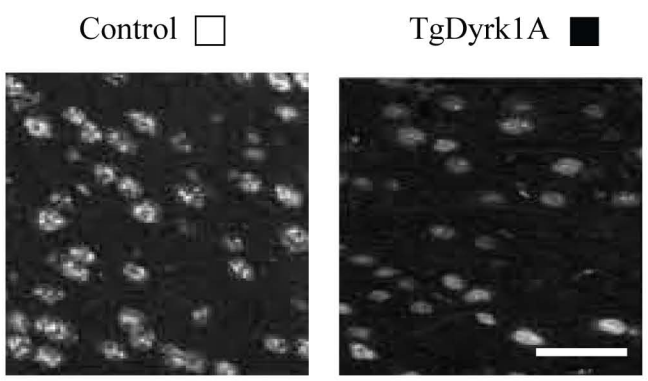
Control
TgDyrk1A

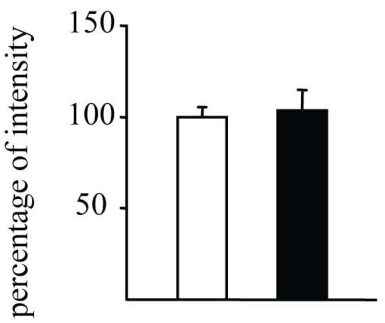
percentage of intensity
150
100
50

E

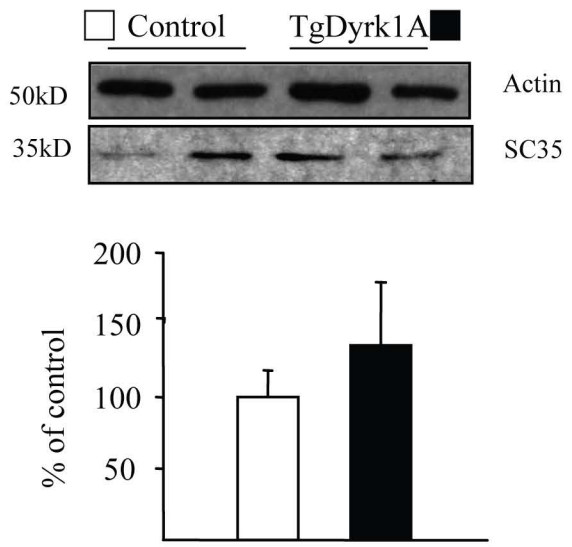
Control
TgDyrk1A
50kD
35kD
Actin
SC35
% of control
200
150
100
50

F

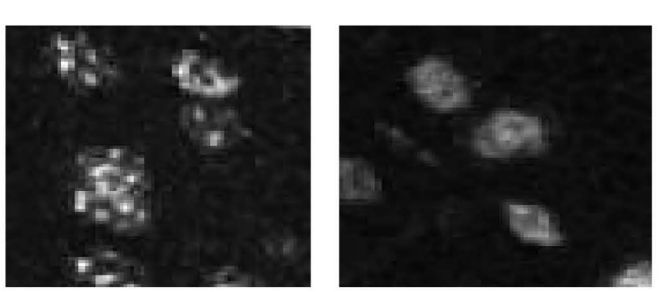
Control
TgDyrk1A

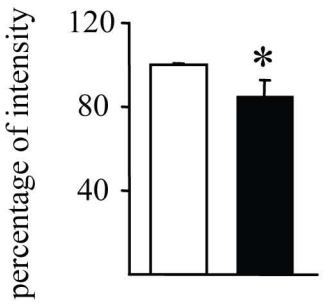
percentage of intensity
120
80
40
*

A

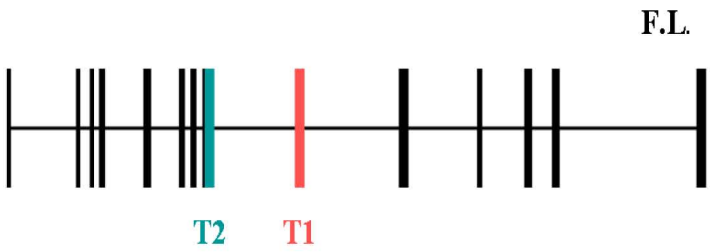
F.L.
T2
T1

B

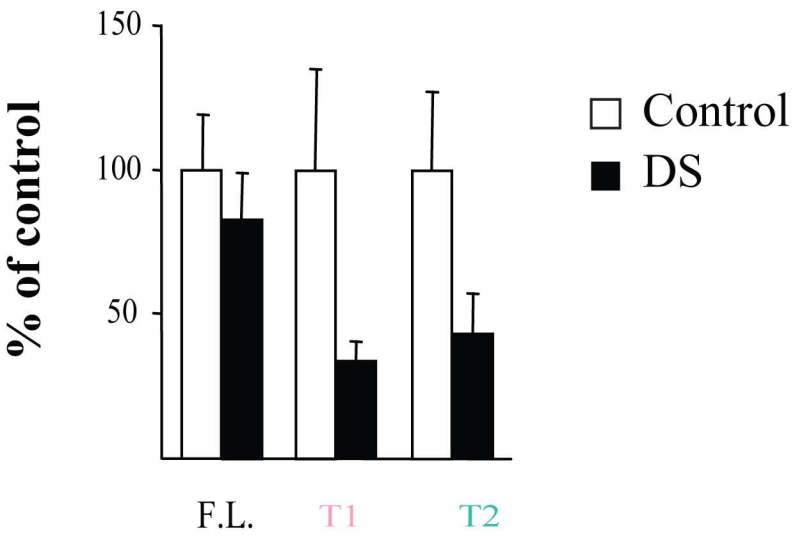
150
100
50
% of control
Control
DS
F.L.
T1
T2

C

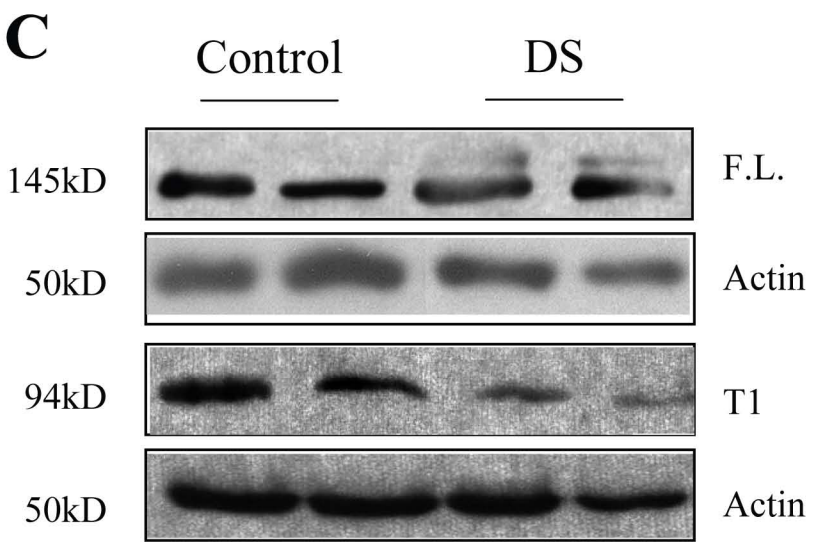
Control
DS
145kD
F.L.
50kD
Actin
94kD
T1
50kD
Actin

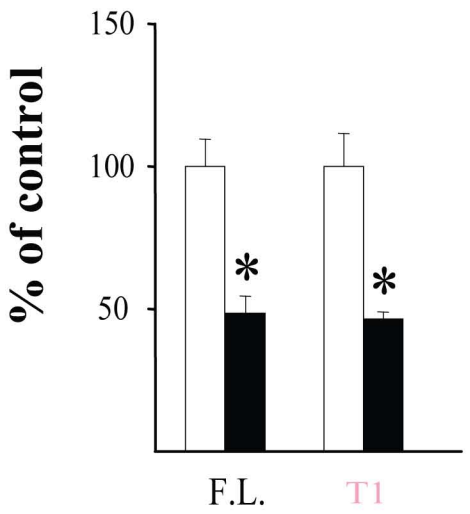
150
100
50
% of control
*
*
F.L.
T1

D

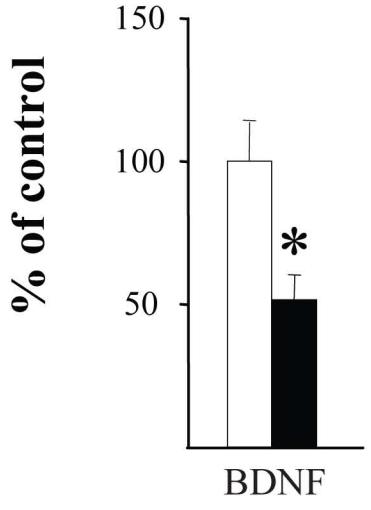
150
100
50
% of control
*
BDNF

E

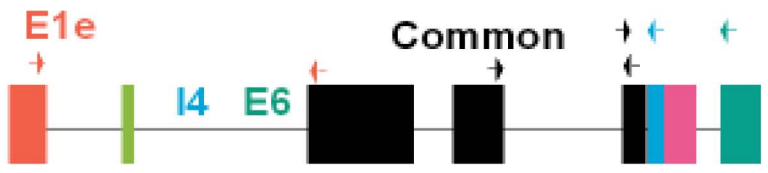
E1e
Common
I4
E6

G

F

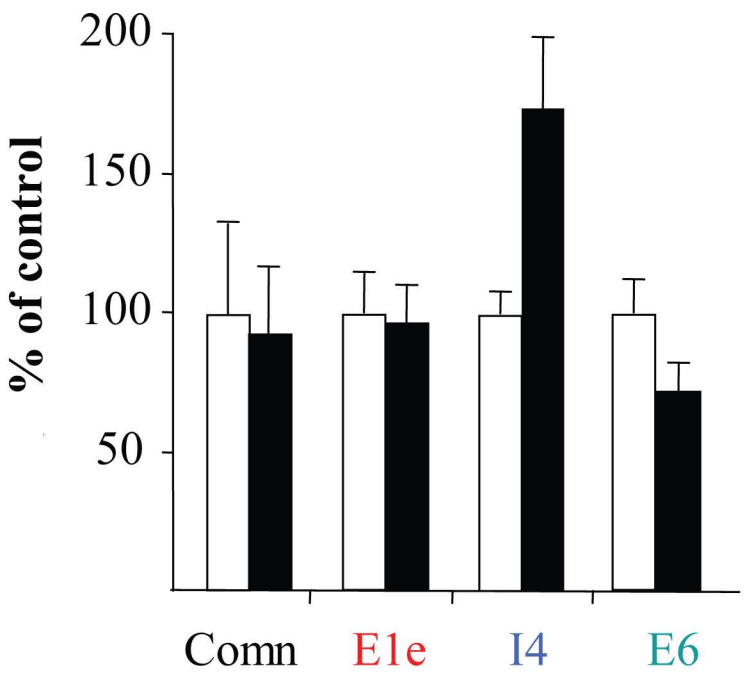
200
150
100
50
% of control
Comn
E1e
I4
E6

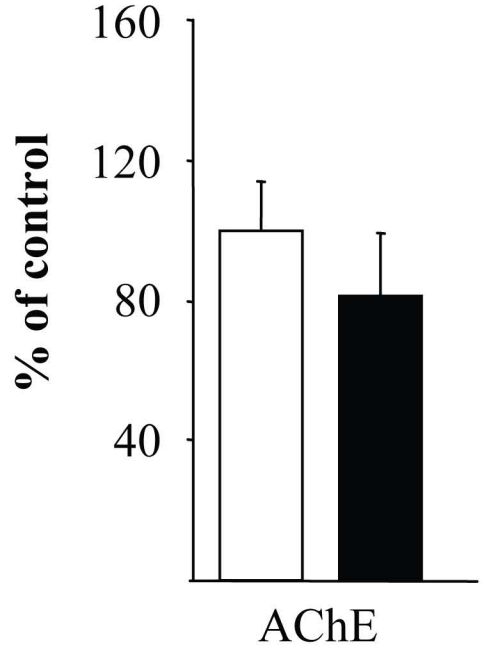
160
120
80
40
% of control
AChE

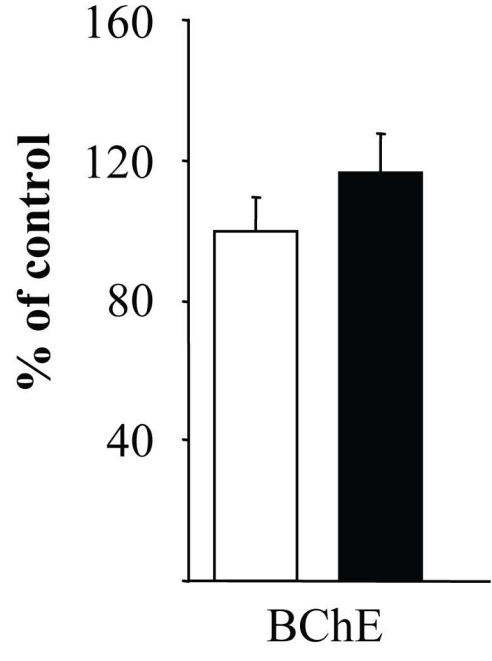
160
120
80
40
% of control
BChE

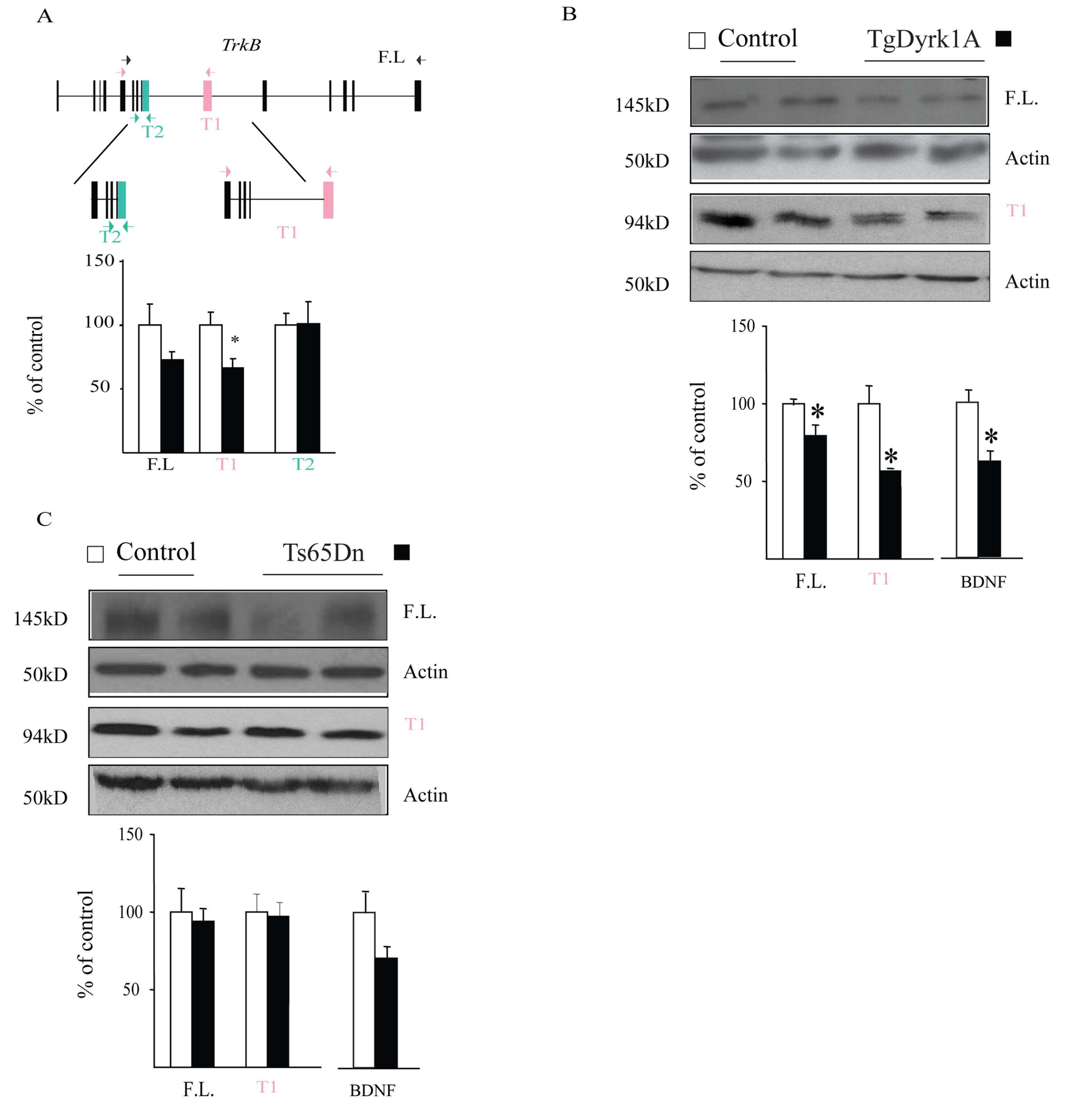
A
TrkB
F.L
T2
T1
T2
T1
150
100
50
% of control
*
F.L
T1
T2
B
Control
TgDyrk1A
145kD
F.L.
50kD
Actin
94kD
T1
50kD
Actin
150
100
50
% of control
*
*
*
F.L.
T1
BDNF
C
Control
Ts65Dn
145kD
F.L.
50kD
Actin
94kD
T1
50kD
Actin
150
100
50
% of control
F.L.
T1
BDNF

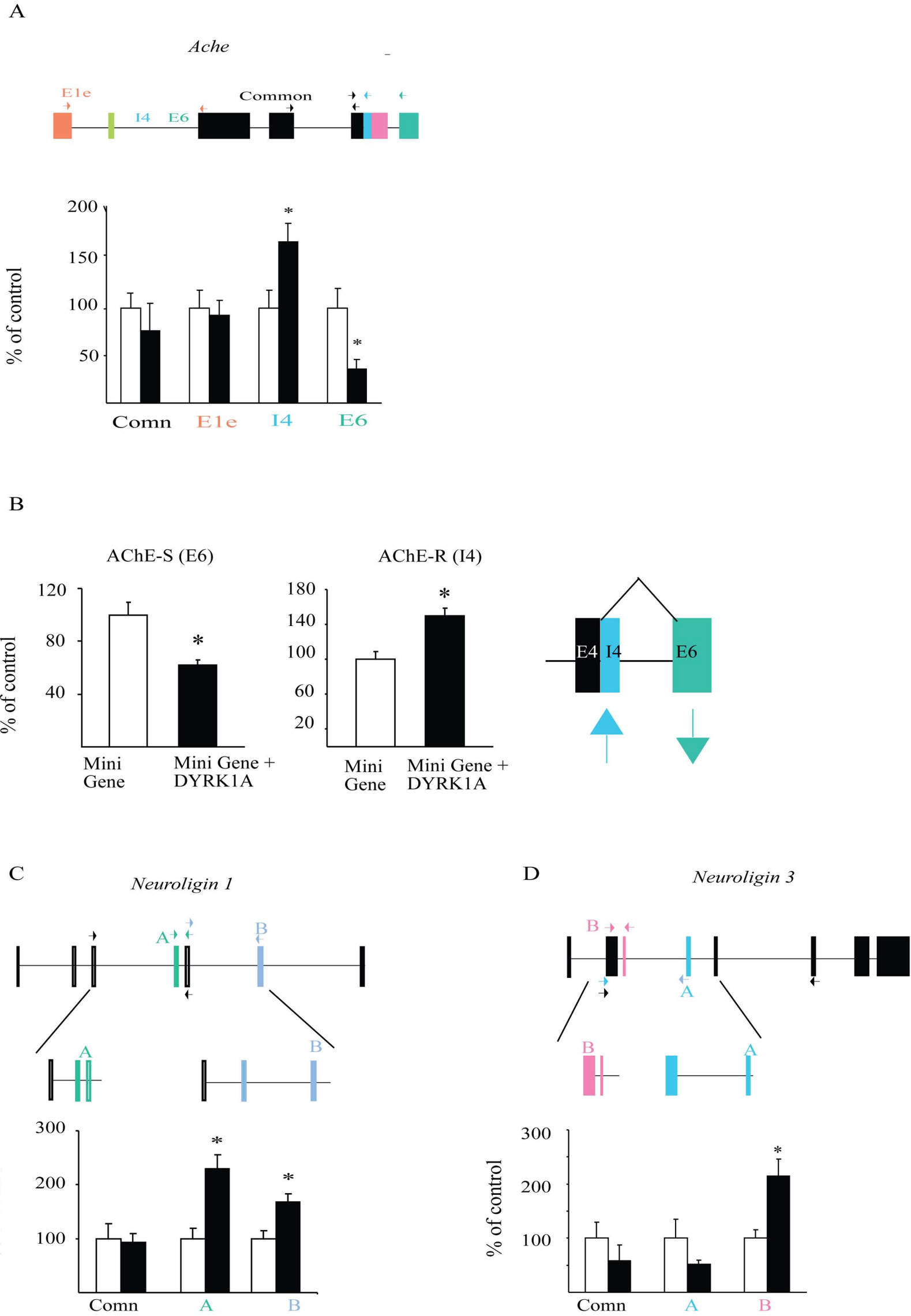
A
Ache
E1e
Common
I4
E6
200
150
100
50
% of control
*
*
Comn
E1e
I4
E6
B
AChE-S (E6)
AChE-R (I4)
120
80
40
180
140
100
60
20
% of control
*
*
Mini Gene
Mini Gene + DYRK1A
Mini Gene
Mini Gene + DYRK1A
E4
I4
E6
C
Neuroligin 1
A
B
A
B
300
200
100
% of control
*
*
Comn
A
B
D
Neuroligin 3
B
A
B
A
300
200
100
% of control
*
Comn
A
B

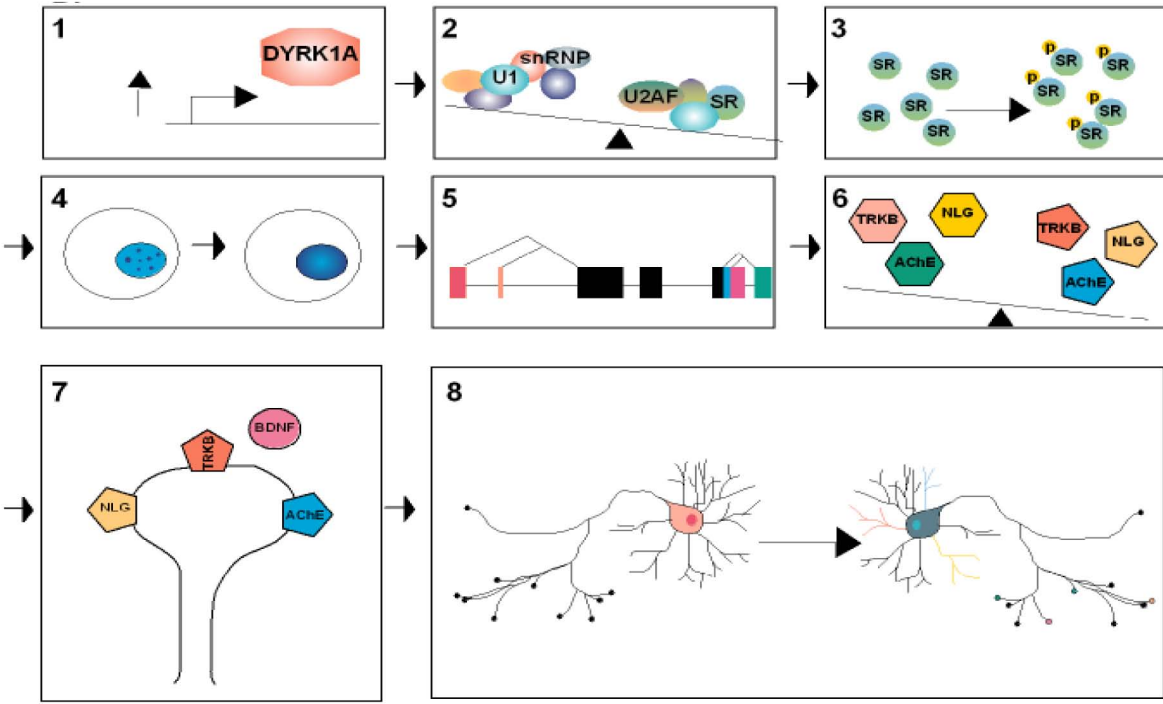
1
DYRK1A
2
snRNP
U1
U2AF
SR
3
SR
P
4
5
6
TRKB
NLG
AChE
7
BDNF
8

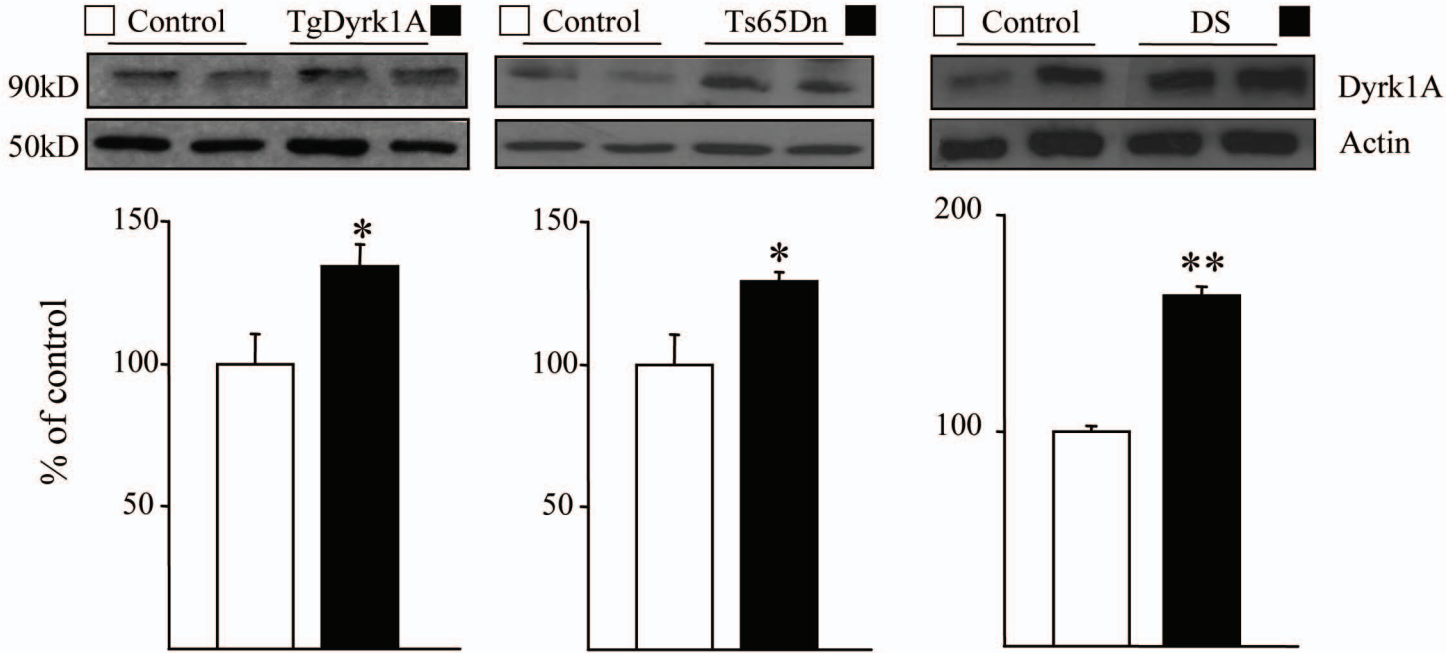
Control
TgDyrk1A
Control
Ts65Dn
Control
DS
90kD
50kD
Dyrk1A
Actin
% of control
150
100
50
*
150
100
50
*
200
100
**

Transcript ID	Exp1	Exp2
target genes		
Mfap1_alt2	-0.812	-0.29
Aqp4_com	-0.631	-0.312
Ars2-pending	-0.5	-0.296
Mapk8	-0.271	-0.077
Pdyn_old	-0.244	-0.18
Clcn3_alt2	-0.148	-0.224
Mfap1_alt1	0.361	0.113
ARS2_alt1	0.376	0.119
PenK1_old	0.517	0.211
apoptosis		
bax_alpha	-0.361	0.112
ICAD_com	-0.289	0.136
casp2_com	-0.176	-0.131
casp2_alt	-0.149	-0.07
Bid	0.095	-0.151
bcl-X_com	0.291	0.091
Ctnnbl1 (NAP)	0.929	-0.079
madd_com	1.215	0.419
Bcl2l13	1.31	0.232
cholinesterase		
Pon1	-0.849	-0.258
mE1c	-0.677	-0.175
Ache-mE2	-0.517	0.235
Pon3	-0.29	-0.24
mE3	-0.242	0.157
Pon2	0.002	-0.078
BChE	0.846	0.235
BCHE-old	1.151	0.198
helicases		
Ddx46	-0.875	-0.305
Ddx27_alt1	-0.14	-0.139
Bat1a	0.217	-0.168
Ddx41	0.295	0.313
ddx48	0.351	0.286
KIAA-homolog	0.363	0.135
Ddx5 (p68)	0.66	0.371
Ddx27_com	1.25	0.221
spliceosome assembly		
gemin2 (sip1)	-0.643	-0.28
gemin3_alt	-0.573	-0.236
Plrg1	-0.383	-0.116
Gemin7	-0.354	-0.212
Cdc5l	-0.189	0.604
gemin4	-0.021	-0.152
SKIIP	0.425	-0.18
Sart1	0.536	-0.071
SR and SR-RELATED		
tra2beta_alt3	-0.373	-0.114
SRp55 (sfrs6)-penc	-0.125	-0.213
SC35-old	-0.118	-0.154
tra2beta_alt1	0.025	-0.132
SRp40 (sfrs5)	0.511	0.889
tra2beta_alt2	0.516	0.572
SRp54	0.639	0.252
ASF/SF2 (sfrs1)	0.708	0.453

Transcript ID	Exp1	Exp2
hnRNPs		
hnRNP K_Pcom	-0.407	0.071
hnRNP A1	-0.128	0.137
snRNP E	-0.071	-0.084
hnRNP K_alt1	-0.044	-0.275
ptbp1_alt2	0.053	-0.149
hnRNP C	0.162	0.125
Ptbp1_alt1	0.162	0.118
brPTB (ptb2)	0.192	-0.169
Pcbp2_com	0.4	0.419
hnRNP K_alt2	0.407	0.573
hnRNP L-old	0.477	-0.095
hnRNP K_alt3	0.578	-0.088
hnRNP H1	1.449	0.318
house-keeping genes		
Rl13a	-0.574	-0.266
atubulin4	-0.404	-0.138
Ndufc1	-0.242	0.078
atubulin1	1.431	0.218
mRNA processing		
Cpsf4	-0.336	0.125
NLP4	-0.166	0.264
cstf3_com	-0.163	0.208
Refbp2	0.685	-0.198
Pabpc1	1.395	0.298
other spliceosomal component		
Wtap	-0.51	-0.174
Ayelet 4	-0.398	-0.247
Wbp11	-0.274	-0.138
Rnpc2	-0.111	-0.034
Bcas2	-0.074	-0.17
Cd2bp2	0.045	0.089
SMNRP(sf30)	0.239	0.246
sam68(Khdrbs1)	0.604	0.522
RBM17	0.92	-0.18
snRNPs		
U4/U6-20kD-pending_	-0.439	-0.214
snRNP D1-old	-0.109	-0.139
U1snRNP70_com	0.253	-0.115
U5 116 kd-old	0.301	0.12
U2A'-old	0.329	-0.105
snRNP d3	0.581	0.464
sf3b1 (SAP155)	0.592	-0.139
Lsm4	0.677	0.284
U4/U6-20kD-pending_	0.685	0.246
snRNP N_alt1	1.409	-0.063
splicing factors phosphorylation		
Clk3_com	-0.476	-0.103
Prpf4b_com	-0.418	0.303
Clk3_alt	-0.332	0.37
Clk2	-0.294	-0.1
Prpf4b_alt2	-0.199	0.262
pp2r2b	0.182	0.043
Prpf4b_alt1	0.228	0.145
Ppp2r5e	0.293	0.188
Clk1 (sty)	0.557	-0.085
Ppm1g (pp2c)	0.624	0.174

-0.9
-0.7
-0.5
-0.3
-0.2
0
0.2
0.4
0.6
0.8
1
1.3
1.5

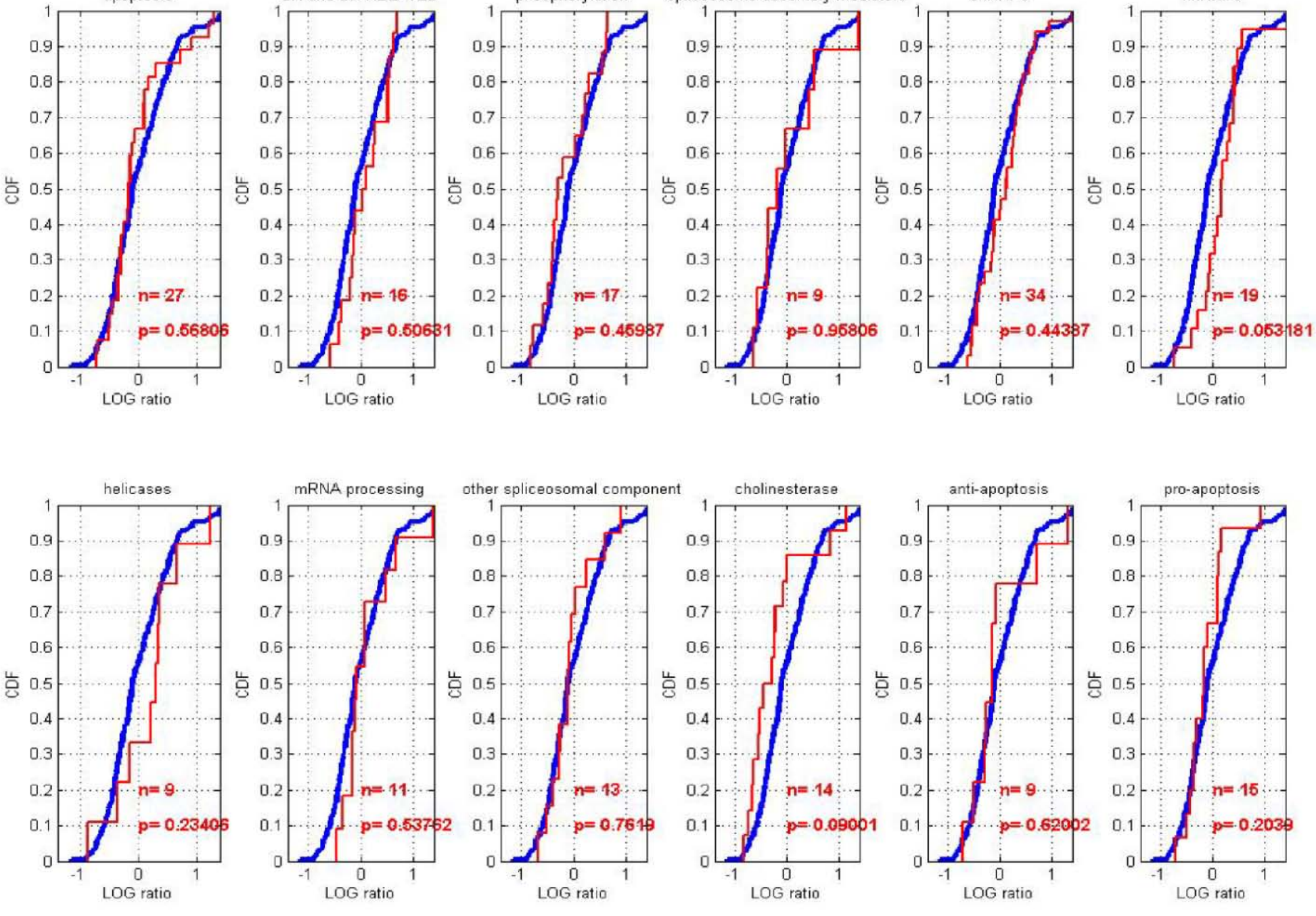
apoptosis
n= 27
p= 0.56805
SR and SR RELATED
n= 16
p= 0.50631
phosphorylation
n= 17
p= 0.45937
spliceosome assembly mediators
n= 9
p= 0.95806
snRNPs
n= 34
p= 0.44387
hnRNPs
n= 19
p= 0.053181
helicases
n= 9
p= 0.23406
mRNA processing
n= 11
p= 0.53762
other spliceosomal component
n= 13
p= 0.7619
cholinesterase
n= 14
p= 0.09001
anti-apoptosis
n= 9
p= 0.62002
pro-apoptosis
n= 15
p= 0.2039
CDF
LOG ratio